MARCH 2016 VOL 9 NO 3
www.nature.com/naturegeoscience

nature geoscience

GIANT ICEBERGS
Ocean productivity boost

LATE ANTIQUE UPHEAVAL
Cooling and societal change

SNOWBALL OCEANS
Ridge volcanism influence

Continents created from reprocessed magmas

nature geoscience

REVIEW ARTICLE

PUBLISHED ONLINE: 22 FEBRUARY 2016 | DOI: 10.1038/NGEO2662

Formation of lower continental crust by relamination of buoyant arc lavas and plutons

Peter B. Kelemen[1] and Mark D. Behn[2]

The formation of the Earth's continents is enigmatic. Volcanic arc magmas generated above subduction zones have geochemical compositions that are similar to continental crust, implying that arc magmatic processes played a central role in generating continental crust. Yet the deep crust within volcanic arcs has a very different composition from crust at similar depths beneath the continents. It is therefore unclear how arc crust is transformed into continental crust. The densest parts of arc lower crust may delaminate and become recycled into the underlying mantle. Here we show, however, that even after delamination, arc lower crust still has significantly different trace element contents from continental lower crust. We suggest that it is not delamination that determines the composition of continental crust, but relamination. In our conceptual model, buoyant magmatic rocks generated at arcs are subducted. Then, upon heating at depth, they ascend and are relaminated at the base of the overlying crust. A review of the average compositions of buoyant magmatic rocks — lavas and plutons — sampled from the Aleutians, Izu–Bonin–Marianas, Kohistan and Talkeetna arcs reveals that they fall within the range of estimated major and trace elements in lower continental crust. Relamination may thus provide an efficient process for generating lower continental crust.

Arc magmatism is thought to have played a central role in creating continental crust because magmatic rocks — erupted as andesitic lavas and intruded to form plutons — found in subduction-related volcanic arcs have compositions that closely resemble bulk continental crust (BCC) and lower continental crust (LCC)[1–5]. Some arc magmas resemble continental crust because they include a recycled component from subducted, continentally derived sediments. But other arc lavas that lie within the compositional range of estimated BCC and LCC are the most isotopically depleted arc magmas worldwide, indicating that they contain little or no contribution from recycled, older continental material[6,7]. Thus, juvenile igneous material with the major and trace element composition of continental crust is extracted directly from the Earth's mantle by arc magmatic processes.

Although arc magmatism must play a key role in forming continental crust, arc lower crust is systematically depleted in highly incompatible elements compared with all estimates for LCC (Fig. 1). To address this discrepancy, here we quantify the marked differences in trace elements between arc lower crust and LCC. We then review how density sorting processes in which dense lithologies descend into the less dense mantle, while buoyant lithologies ascend to become part of the lower crust, might form LCC. We use constraints from trace element measurements to show that a single stage of delamination of dense lithologies from the base of arc lower crust cannot transform arc lower crust into LCC. Instead, relamination — in which subducting, buoyant arc crustal material detaches from denser material and rises, relaminating the base of the overlying crust — can quantitatively reproduce the composition of LCC. We calculate densities for arc lava and pluton compositions at subduction zone pressures and temperatures, and compare them to upper mantle peridotite under the same conditions. We show that the average composition of buoyant arc material is within the range of estimates for LCC for both major and trace elements. Thus, relamination of subducted, buoyant arc magmas provides a simple, quantitative model for the formation of continental lower crust.

Composition of continental crust

The continental crust has an average thickness of ~40 km and may be broadly divided into upper, middle and lower layers, each comprising about a third of the total thickness[8–11]. In general, upper continental crust (UCC) is much better sampled, and probably more SiO_2-rich, than middle and lower crust. It is unclear whether there is a compositional distinction between the middle and lower layers[12]. As a result, and for simplicity, in this paper we consider LCC to represent the lower half of BCC, extending from ~20 to 40 km depth.

Two types of samples may be representative of LCC: regional metamorphic massifs whose mineral assemblages record lower crustal pressure (0.5 to 1.5 GPa), and metamorphic rock fragments carried to the surface in continental volcanic centres (xenoliths). Early estimates of LCC focused on metamorphic massifs, which have andesitic average SiO_2 contents of ~60 to 65 wt%. A series of influential papers by Rudnick and co-workers[2,11,13–15] argued that metamorphic xenoliths[15,16] are more representative of LCC. These samples have basaltic compositions with average SiO_2 ~52 wt%. In this view, the average xenolith composition provides a better fit to seismic and heat flow constraints on LCC. Recent reanalysis indicates, however, that a broad range of estimated LCC compositions, including estimates based on metamorphic massifs[12,17,18], are consistent with these geophysical observations.

Regardless of whether it is basaltic or andesitic, LCC has trace element contents similar to BCC (Fig. 1 and ref. 19). LCC and BCC are rich in incompatible elements — those elements that preferentially remain in melt during crystallization and partial melting. LCC concentrations are within a factor of three of BCC for almost all elements plotted in Fig. 1a. Among proposed LCC compositions, those derived from metamorphic xenolith averages[11,13,14] are the most depleted in incompatible elements. These are based largely on data compiled by Rudnick and Presper[15]. An updated xenolith compilation[16] is less depleted, and more similar to BCC. All other LCC estimates, mostly derived from metamorphic massifs, are even closer to BCC.

[1]Department of Earth and Environmental Sciences, Columbia University, LDEO, Palisades, New York 10964, USA. [2]Department of Geology and Geophysics, Woods Hole Oceanographic Institute, Woods Hole, Massachusetts 02543, USA. e-mail: peterk@LDEO.columbia.edu; mbehn@whoi.edu

NATURE GEOSCIENCE DOI: 10.1038/NGEO2662

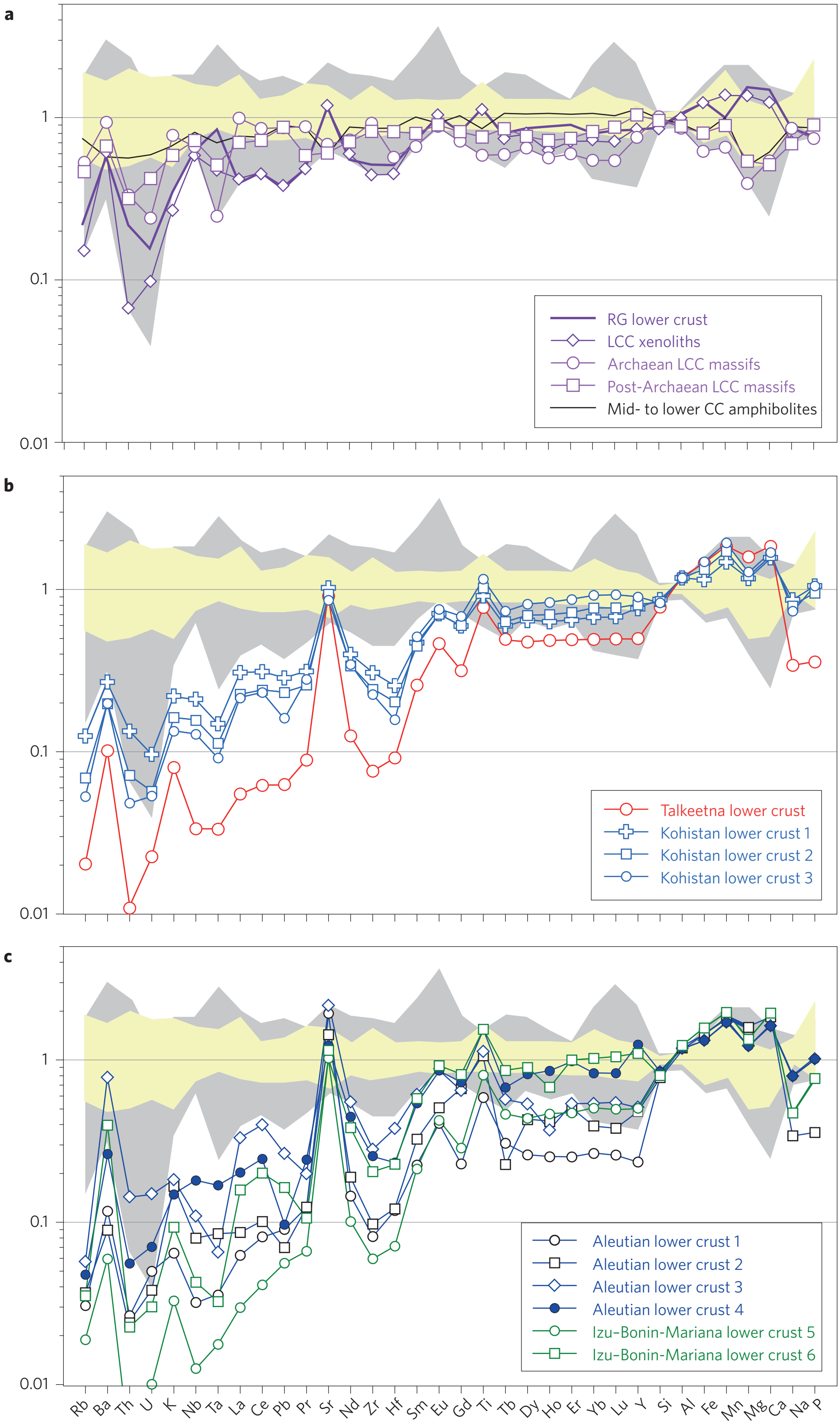

Figure 1 | Comparison of trace elements in arc versus continental lower crust. Log-normal average arc compositions are compared with upper- and lower-bound estimates of bulk continental crust (BCC, yellow field) and lower continental crust[1,11–14] (LCC, grey field) normalized to BCC composition, from refs 13,14. Supplementary tables provide linear average and median values. **a**, Continental lower crust compositions normalized to BCC. RG (Rudnick and Gao) lower crust (heavy purple line) is an LCC estimate[11,13,14] based largely on a metamorphic xenolith compilation[15]; thin purple lines with symbols, updated metamorphic massif and xenolith compilations[12,16]. **b**,**c**, Arc lower crust compositions normalized to BCC. **b**, Observed arc lower crust from the Talkeetna and Kohistan arcs (Talkeetna: major elements from composition 2a, ref. 83; trace elements from ref. 7; Kohistan: results from ref. 21). **c**, Aleutian and IBM lower crust compositions[6,7,39,79,84,85]. Compositions estimated as described in the Supplementary Information.

Comparing arc lower crust and LCC compositions

In contrast to andesitic lavas and mid-crustal plutons in arcs, arc lower crust is very different from BCC and LCC (Fig. 1 and Supplementary Fig. 1). Figure 1b shows this for trace elements in exposed lower crust from two tectonically accreted arc sections, the Jurassic Talkeetna arc in south central Alaska[6,7,20] and the Cretaceous Kohistan arc in northern Pakistan[21]. Similarly, Fig. 1c illustrates estimated lower crust compositions in the circum-Pacific Aleutian and Izu–Bonin–Mariana volcanic arcs.

Concentrations of Ta, K, La, Ce and Hf show the largest difference between arc lower crust and LCC (Fig. 2 and Supplementary Fig. 2). Most samples of arc lower crust are depleted in these elements compared with most LCC samples from both metamorphic xenoliths and massifs. This is true despite the fact that the Talkeetna arc section is thought to have undergone delamination of low-SiO_2 lithologies such as primitive pyroxenite and garnet[6,7,22,23]. It is also true of relatively buoyant, garnet-free, low-SiO_2 Kohistan gabbroic rocks, as well as dense garnet-bearing metamorphic rocks deeper in the Kohistan section.

Creating andesitic igneous rocks in arcs

As noted above, BCC and most estimates for LCC are strikingly similar to andesitic igneous rocks with 54 to 65 wt% SiO_2, particularly to andesites with high magnesium number (molar Mg/(Mg+Fe), or Mg#)[1] in the range 0.43 to 0.55 (Supplementary Fig. 1). Trace elements in high-Mg# andesites are also very similar to BCC and LCC (Supplementary Fig. 1). Such igneous rocks are characteristic of arcs, and rare in other tectonic settings. This suggests that formation of high-Mg# andesites in arcs plays a key role in continental genesis[1–5]. In contrast, mid-ocean-ridge basalts, with 48 to 52 wt% SiO_2, are strikingly depleted in incompatible elements compared with BCC and LCC, as are average arc lavas, which include abundant basalts as well as high-Mg# andesites (Supplementary Fig. 1).

As stated above, although the composition of some arc magmas is influenced by recycling of components from subducted, continentally derived sediments, other arc magmas — including many high-Mg# andesites — are juvenile, with isotope characteristics indicating that they were derived from the mantle, with little or no recycling of older continental material[6,7] (Supplementary Fig. 3). In explaining the origin of continental crust, we cannot call upon recycling of continental crust. Thus, to develop a simple, uniformitarian hypothesis for the origin of continental crust, we focus on juvenile igneous rocks from arcs.

Many explanations have been offered to explain the genesis of juvenile, high-Mg#, andesitic rocks in arcs (Supplementary Fig. 4; Supplementary Table 2; also see Fig. 14 in ref. 24). These include crystallization of a relatively low-Si, high-Fe mineral assemblage, rich in Fe–Ti oxides and/or aluminous hornblende from primitive basalt with high H_2O content and oxygen fugacity fO_2 (refs 25–27); crystallization of parental, primitive andesite[1,26,28,29]; and/or mixing of basaltic magma with granitic magma[30,31] (SiO_2 > 70 wt%, Mg# < 0.3). In the case of continental crust, the third option could also take the form of mechanical juxtaposition of solid basalt and granite.

To form an andesitic BCC and LCC through any of these processes requires removal of SiO_2-poor and incompatible-element-poor crystalline products (proportions in Supplementary Table 2), or modification by chemical weathering. Below we focus on density sorting processes that remove SiO_2-poor lithologies from the crust. Here we briefly consider — and reject — the alternative that weathering converts basaltic arc crust to andesitic continental crust[32,33]. Subaerial leaching of basaltic crust removes K and Na relative to Mg and Fe, and removes more Mg than Fe (at least, at high fO_2 since ~2 billion years (Gyr) ago), providing a poor match for the alkali-rich, high-Mg# composition of continental crust[1]. Oxidative seafloor weathering may have delivered higher alkali contents, with higher K/Na, to the arc magmatic source since ~2 Gyr ago[34,35] but — given the similarity of Archaean and post-Archaean BCC[4,5,36], and of Archaean and post-Archaean metamorphic terrains[12,15,16] — this has been a minor effect. Mechanical erosion may preferentially remove lavas, exposing plutonic rocks that are more resistant. In arcs such as the Aleutians, more than half the lavas are basaltic, whereas mid-crustal plutons are relatively SiO_2-rich (see average pluton in Supplementary Fig. 1, Supplementary Table 1 and refs 6,7,37–39). Even so, to transform basaltic arc crust to high-Mg#, andesitic continental crust, additional processes must remove SiO_2-poor sediments and lower crust, an inference that is consistent with evidence from trace element ratios[40,41].

Density sorting processes in arcs

Removal of SiO_2-poor, basaltic compositions from arc crust to produce continental crust could occur via density instabilities. At temperatures >700 to 800 °C, compositional density contrasts of 50 to 200 kg m^{-3} in layers more than ~100 m thick form diapirs that move through mantle peridotite on timescales that are rapid relative to subduction rates[42–44]. This can drive (1) delamination of dense lithologies into less dense, underlying mantle[43,45–47], and/or (2) relamination of buoyant material, which is subducted and then ascends (along a subduction channel or in diapirs) to the base of the overlying crust[18,42,48–50].

Evidence for delamination includes a compositional gap between crystalline products of mantle-derived magmas, with Mg# ≈ 0.9, and primitive igneous rocks in arc lower crust, with Mg# ≈ 0.8 (refs 6,21). The few rocks with 0.8 < Mg# < 0.9 are pyroxenites and garnet-rich lithologies that are denser than mantle peridotite at the same pressure and temperature[51]. It is proposed that 25–60% of magmatic arc crust was composed of dense rocks that foundered into the underlying mantle[6,52]. Other evidence for delamination includes seismic data and xenolith compositions, for example in the Sierra Nevada where there is an abrupt P-wave velocity increase from low, granitic values to mantle peridotite values, and Miocene xenoliths include abundant, dense, garnet pyroxenites that are absent from younger xenolith suites[53,54].

Evidence for relamination is provided by high- and ultrahigh-pressure metamorphic rocks, which are subducted to depths >40 km (>100 km for ultrahigh pressure) and then returned to the base of the crust (~35 km) prior to later exhumation[18,55]. Moreover, distinctive peraluminous metasediments are common in lower continental crust[12,18], perhaps as a result of relamination. Underplating of buoyant lithologies at the base of the crust above subduction zones can occur by imbrication, flow up a subduction channel, or diapirs rising through the mantle wedge (Supplementary Fig. 5). Imbrication of subducting trench sediments is observed in metamorphic terrains[56] and inferred from seismic data[57,58]. Ultrahigh-pressure rocks provide clear evidence for ascent in a subduction channel[59,60]. Efficient recycling of subducted sediment components into some arc magmas[42], and grospydite xenoliths derived from metasediments but recording mantle wedge pressure and temperature[61], are consistent with formation and melting of metasedimentary diapirs rising through the mantle wedge.

Relamination of buoyant magmatic rocks may be common. It is difficult, however, to determine the provenance of quartzo-feldspathic gneisses, unlike peraluminous metasedimentary compositions that are easily identified in metamorphic suites. Quartzo-feldspathic gneisses could be derived from plutonic rocks, lavas, pyroclastic deposits or volcanoclastic sediments. Archaean and post-Archaean metamorphic terrains are dominated by quartzo-feldspathic gneisses with andesitic compositions, which could have been relaminated as described above. A clear example is a remnant of jadeite granite in the western Alps[62], which preserves high-pressure mineral parageneses, within a larger mass of rocks of andesitic composition whose high-pressure history was obliterated during retrograde metamorphism.

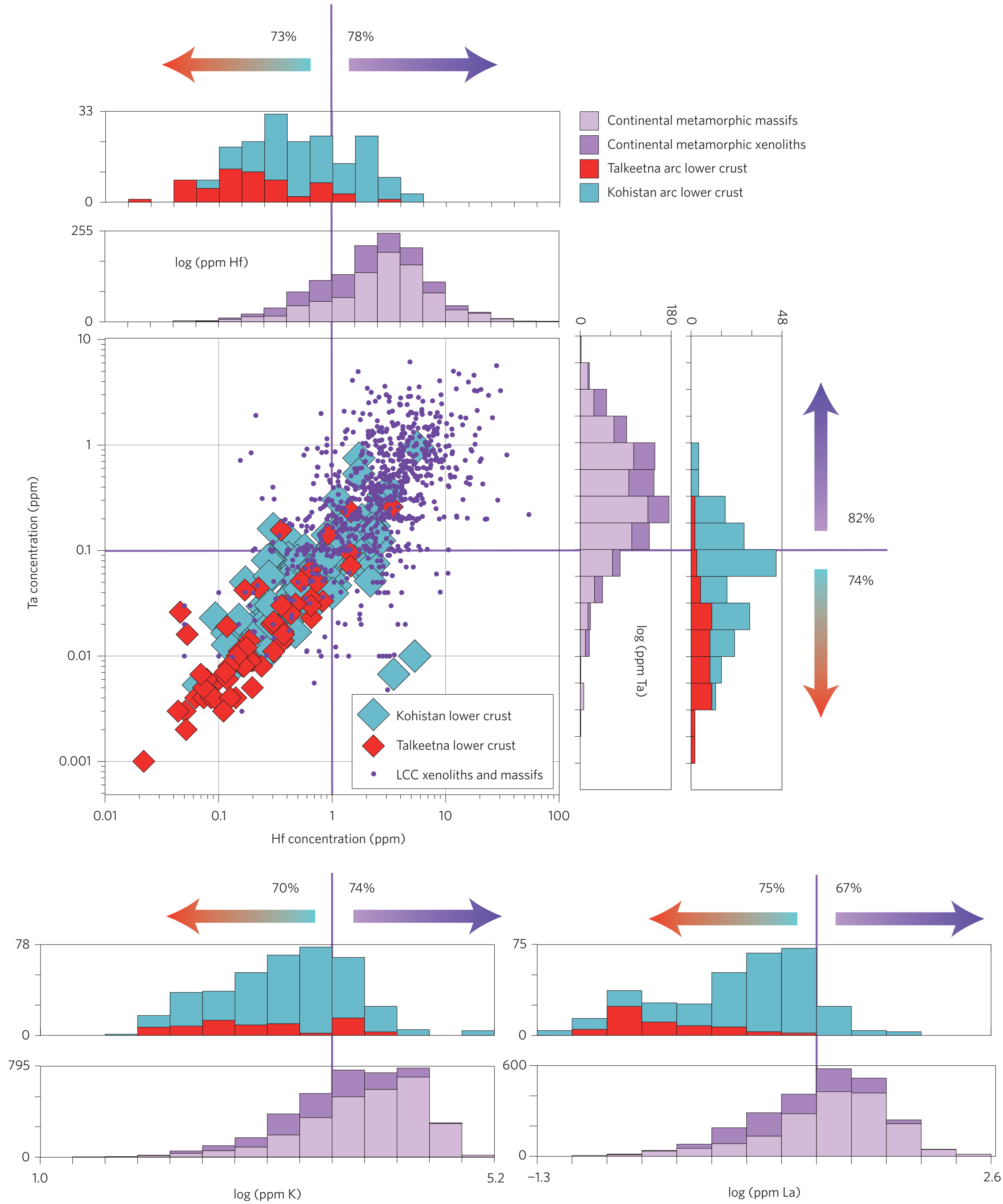

Figure 2 | Incompatible element concentration in LCC and in Talkeetna and Kohistan arc lower crust. Concentrations of Ta, K, La and Hf in Talkeetna and Kohistan arc lower crust are systematically lower than in LCC as represented by continental metamorphic xenoliths and massifs. Data sources as for Fig. 1. See Supplementary Fig. 3 for cross plots of La, Ce and K. Compositions of Kohistan ultramafic rocks (SiO_2-poor rocks with no plagioclase feldspar) at depths greater than 55 km are not plotted. Histograms plot number of samples versus element concentration. Horizontal axis values in histograms are minimum and maximum concentrations in log (ppm) units. Arrows above histograms indicate the proportion of arc lower crust to the left of the bold dividing lines (blue to red), and the proportion of LCC samples to the right of the line (purple).

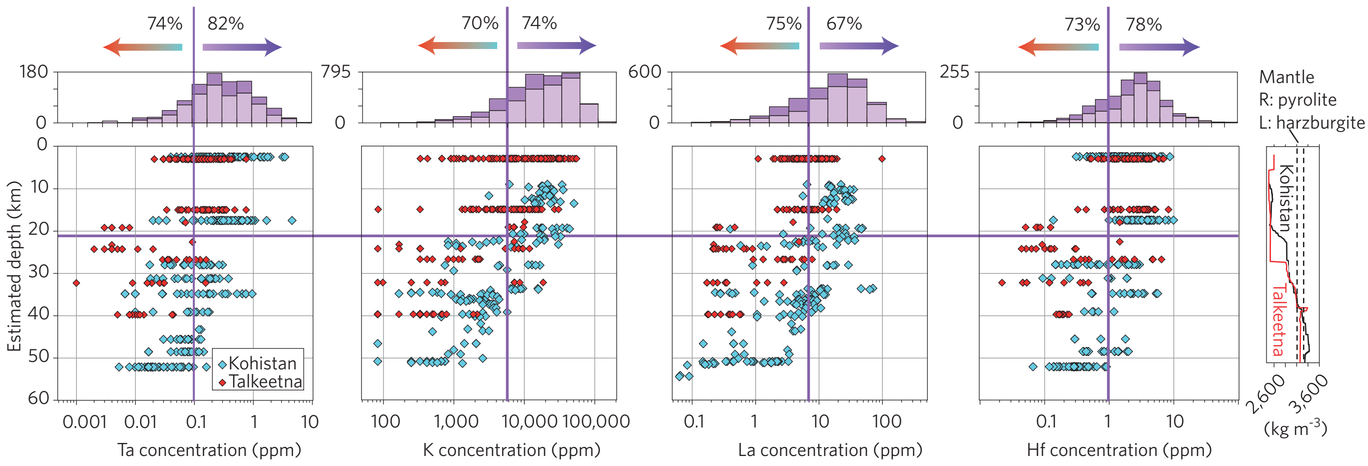

Figure 3 | Incompatible trace-element concentration in Talkeetna and Kohistan arc crust as a function of depth. Compiled pressure–depth estimates and compositions for Talkeetna[7] and Kohistan[86]. Most arc samples with Ta, K, La and Hf concentrations comparable to LCC are in the upper 20 km of arc crust. Right inset shows calculated densities for Talkeetna and Kohistan sections[86]. Compositions of Kohistan ultramafic rocks at >55 km depth are not plotted. The horizontal line just below 20 km depth separates crustal levels with average rock concentrations similar to LCC, above, from levels with rock concentrations lower than LCC, below. Colours of symbols (Talkeetna, red; Kohistan, blue) and histogram bars (LCC massifs, light purple; LCC xenoliths, dark purple) correspond to those in Figure 2. Arrows and percentage values indicate the proportion of arc lower crust (red-blue arrows) and LCC (purple arrows), left and right of the bold dividing line, respectively, as in Figure 2. In the inset, vertical dashed lines indicate density of fertile mantle peridotite (pyrolite) on the right (R), and a residual mantle peridotite after extensive melt extraction (harzburgite) on the left (L).

Mass balance for relamination versus delamination

Crustal differentiation by relamination is more efficient than delamination. To create andesitic BCC by delamination of SiO_2- and incompatible-element-poor components from arc lower crust by the mechanisms described above requires removal of 25–89% of the mass of magmas forming arc crust (Supplementary Table 2; refs 40,52). To do this by means of delamination would require repeated crustal thickening and metamorphic events, with each event forming and removing dense, garnet-bearing metamorphic rocks from a narrow depth interval near the base of the crust. By contrast, subduction transports all lithologies to pressures of 2 GPa or more, where dense, metamorphic garnet is stable — implying that density sorting by means of relamination could occur in a single stage.

For example, to eliminate lithologies with low Ta, K, La and Hf from Talkeetna and Kohistan arc lower crust, and preserve lithologies with the higher concentrations characteristic of LCC, delamination would have to remove most of the rocks at depths >20 km in those sections (Fig. 3). But low-SiO_2, gabbroic arc lithologies are only denser than mantle peridotite when they form abundant garnet, at depths >35 km (Fig. 3 inset)[12,29,43,51]. In contrast, if subduction erosion carried the Talkeetna and Kohistan crust to >700 °C at 2–4 GPa (in subduction zones, or by imbrication into hot, arc lower crust) then density sorting would efficiently concentrate buoyant material with high incompatible element concentrations at the base of the overlying crust (Figs 4 and 5), while dense material continued to descend.

Subducted, relaminated rocks may be common in continental lower crust, as suggested by a review[18] of estimates for the rate of (1) sediment subduction (1.1 to 1.6 $km^3\ yr^{-1}$), (2) direct arc subduction (<0.13 to 0.17 $km^3\ yr^{-1}$), and (3) subduction erosion in which sections of arc crust adjacent to the trench are subducted (1.4 to 2 $km^3\ yr^{-1}$)[63,64]. When arcs collide, they may accrete and merge, or one may subduct beneath another[65–69]. If ~17% of subducting sediment is derived from arcs[70], and 20% of arcs subduct during arc–arc or arc–continent collision, then the contribution from subduction erosion is about 7 times as large as that from subduction of arc-derived sediment, and about 60 times as large as the contribution from arc subduction during collisions. If 50% of subducting arc crustal material in all three settings is buoyant (Supplementary Table 3), with an average density (at crustal conditions) of 2.8 to 3.0 tonnes m^{-3}, this is sufficient to relaminate 9–14 × 10^9 gigatonnes of buoyant material over 4 billion years, roughly comparable to the mass of LCC[71].

Of course, global processes are more complex than this, with subduction of buoyant sediments and subduction of continental crust during collisions. But the calculations presented here indicate that arc magmatism, followed by relamination of buoyant, subducting arc magmatic rocks, is sufficient to explain the production of juvenile continental crust.

Arc magmatism plus relamination produces LCC

Here we provide quantitative calculations of the composition of lower crust created by relamination of subducted, buoyant arc lithologies. We begin with a detailed example from the Aleutians.

Aleutian arc lower crust has high seismic wave speeds, implying low SiO_2 (refs 72–74), in keeping with the depleted trace element compositions that we estimate (Fig. 1c, Supplementary Table 1). Thus, despite the similarity of andesitic Aleutian lavas and exposed plutons to BCC and LCC (Supplementary Fig. 1 C,H), bulk Aleutian crust is basaltic and depleted in incompatible trace elements, and requires processing to attain the composition of BCC or LCC. To quantify the potential for relamination to produce LCC, we calculated metamorphic mineral assemblages and densities for Aleutian lava and exposed pluton compositions from the entire oceanic arc (165° W to 164° E) at subduction zone pressures and temperatures using the free-energy minimization code Perple_X[75,76] (methods in Supplementary Information). We then evaluated the composition of material with densities lower than mantle peridotite at the same conditions. Approximately 44% of Aleutian lavas and 78% of exposed Aleutian plutonic rocks are more buoyant than mantle peridotite (pyrolite[77]) along a typical subduction geotherm. Thus, if the Aleutian arc were subducted — by means of subduction erosion, subduction of arc-derived sediment, and/or arc–arc or arc–continent collision — then at a depth of 90 to 120 km (~3–4 GPa) and temperatures >700 °C, lavas and plutons in the top of the subducting arc crust would become sufficiently buoyant, and attain a low enough viscosity, to ascend and accumulate at the base of the overlying crust, as schematically illustrated in Supplementary Fig. 5.

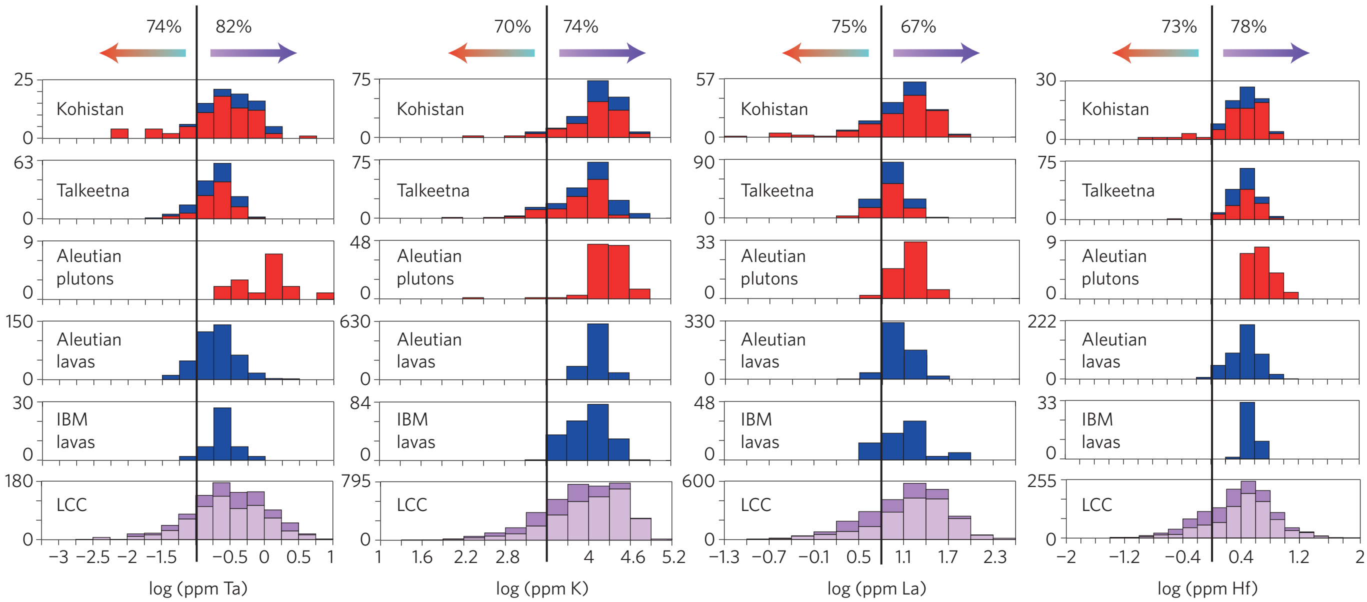

Figure 4 | Incompatible element concentration in arc compositions that are buoyant compared with mantle peridotite. Samples more buoyant than mantle peridotite at subduction zone conditions (Supplementary Table 4) have Ta, K, La and Hf concentrations similar to LCC. This figure shows data from lava (blue) and plutonic (red) samples from Aleutian, Izu–Bonin–Mariana, Kohistan and Talkeetna arcs with densities less than pyrolite at 700 °C, 3 GPa, compared with continental metamorphic xenoliths and terrains[16]. Data as for Fig. 1. Also see Supplementary Fig. 8.

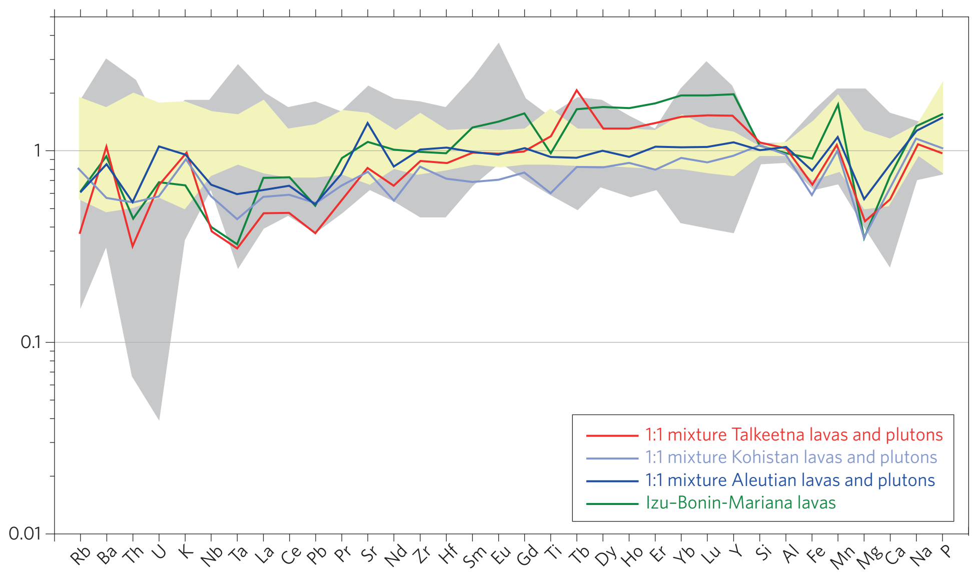

Figure 5 | Compositions of 1:1 mixtures of buoyant lava and plutonic compositions, compared with BCC and LCC. The buoyant arc compositions are normalized to BCC. The figure shows compositions of 1:1 mixtures of log-normal averages of buoyant lava plus plutonic compositions with calculated densities less than pyrolite at 700 °C and 3 GPa, for all arcs discussed in this paper (Supplementary Table 3), compared with BCC (yellow) and LCC (grey). Aleutian and Kohistan compositions lie within the field of LCC for all elements. Talkeetna and Izu–Bonin–Mariana compositions have Nb and Ta concentrations slightly lower than LCC, but are more similar to LCC than arc lower crust in Fig. 1.

For subduction velocities of 0.02 to 0.1 m yr^{-1} and dips of 30 to 60°, buoyant, subducting lithologies will spend 0.4 to 3.5 million years in the depth interval from 90 to 120 km, below typical volcanic arcs. The top of the subducting plate is >700 °C in this depth interval, even for cold subduction zones. Thus, instabilities will form in this depth interval from buoyant layers more than about 100 m thick[42] (Supplementary Fig. 6).

The average buoyant Aleutian lava composition is within the range of LCC estimates for both major and trace elements, except for a slight depletion in Nb (Figs 4, 5, Supplementary Fig. 7 and Supplementary Table 3). Similarly, the average buoyant Aleutian pluton composition is within the range of LCC for all elements we consider, as is a 50:50 mix of buoyant lavas and plutons. Thus, if material from the magmatic Aleutian crust were subducted, and then the buoyant fraction accumulated at the base of the overlying crust, the relaminated material would have the composition of LCC.

Intrigued that subduction and relamination of buoyant Aleutian material provides such a simple explanation for the genesis of LCC, we performed the same calculations for several other arcs. The compositions of lavas, relatively SiO_2-rich plutons and SiO_2-poor lower crust are relatively well known for the Kohistan and Talkeetna sections. Density sorting efficiently removes most samples with low Ta, K, La and Hf (Supplementary Fig. 8). The average of buoyant Kohistan lava compositions is within the bounds for LCC for all elements considered. Buoyant Kohistan pluton compositions are slightly depleted in heavy rare earth elements compared with LCC (Figs 4, 5, Supplementary Fig. 7 and Supplementary Table 3). Average Talkeetna buoyant compositions have Nb and Ta concentrations lower than the minimum estimate for LCC, whereas other elements (except Gd) fall within the bounds for LCC. Low Nb and Ta concentrations could be offset by incorporation of a plume component in continental crust[2,78], and/or accumulation of erosion-resistant rutile and zircon in continental sediments[39]. Nearly half (48%) of Talkeetna lavas and 37% of Talkeetna plutonic rocks are buoyant at depths of 90–120 km in subduction zones, as are 36% of Kohistan lavas and 29% of Kohistan plutonic rocks. Moreover, because many studies of Talkeetna and Kohistan have focused on the lower crust, buoyant, relatively SiO_2-rich plutonic rocks in the upper crust are probably underrepresented in geochemical data compilations. In any case, our results are striking given the substantial differences between LCC and both Kohistan and Talkeetna lower crust (Figs 1 and 2).

We also made calculations for lavas from the well-studied Izu–Bonin–Marianas (IBM) volcanic arc in the western Pacific, south of Japan[79]. IBM lavas are predominantly basalt and basaltic andesite, with depleted trace-element contents intermediate between those of mid-ocean-ridge basalts and BCC (Supplementary Fig. 1). Only 15% of IBM lavas are buoyant with respect to pyrolite. The average of buoyant compositions (Figs 4, 5, Supplementary Fig. 7 and Supplementary Table 3) are similar to those for Talkeetna, and are slightly more depleted than LCC for Nb and Mg. They are, however, substantially closer to LCC than to IBM lower crust prior to density sorting (Figs 1 and 2).

Compatibility with geophysical constraints

Contents of SiO_2 in buoyant lava and pluton compositions from the four arcs discussed here range from 60 to 67 wt%. These are within and just above the range of estimates for BCC (57–65 wt%) and LCC (51–67 wt%)[1,12,13,18]. It is often stated that compositions with >55 wt% SiO_2 have seismic wave speeds at lower crustal depths that are slower than LCC wave speeds[16]. However, proposed LCC compositions with up to 64 wt% SiO_2 satisfy seismic constraints for the LCC[12,17].

Average K_2O, Th and U contents in buoyant arc compositions range from 1.1 to 2.7 wt%, 1.6 to 6.1 ppm and 0.8 to 2.4 ppm, respectively. Most of these are within the bounds for published estimates of BCC (0.9 to 3.5 wt%, 2.9 to 11.2 ppm, 0.7 to 2.3 ppm) and LCC (0.6 to 3.9 wt%, 0.4 to 13.3 ppm, 0.05 to 1.7 ppm)[1,12–14,18]. In one view, the high K, Th and U concentrations in some LCC estimates based on metamorphic massifs may not be compatible with observed heat flow in continental interiors[11,13,14,16]. But LCC composed of post-Archaean metamorphic terrains[15], with 1.5 wt% K_2O, 6 ppm Th and 0.7 ppm U, is consistent with continental heat flow data[18]. More generally, a broad range of compositions of LCC with 52 to 68 wt% SiO_2 satisfies constraints from both seismic data and heat flow[12].

Continental crust formed by relamination

Arc magmatism combined with relamination, as outlined above, could have operated virtually unchanged over much of Earth history to produce continental crust. Although it is uncertain whether subduction operated early in Earth history, it is increasingly clear that the main characteristics of subduction magmatism — hydrous, fluxed melting, with recycling of material descending from the surface of a wet planet — has operated in some form since 4.2 Gyr ago[80,81]. Given the range of estimated, global arc crustal production rates, from 2.0 to 3.8 $km^3 yr^{-1}$ (ref. 82) and the volume of continental crust (~$6.0 \times 10^9 km^3$), all of the continental crust, and a similar volume of subducted, dense residues (~10^9 to $10^{10} km^3$), could have been produced by arc magmatism, followed by subduction and relamination, over the course of Earth history. As a result, there is no obvious requirement for additional mechanisms of continental genesis and growth. Of course, many other processes including delamination, chemical weathering, sediment subduction, intraplate magmatism and other types of relamination have all affected the continents. But these factors may be substantially less important than relamination of subducted, buoyant, andesitic arc material.

Our model of continental crust formation through relamination of buoyant arc magmas has the advantage of simplicity, and fits all known compositional and dynamical constraints. This model can fully explain the composition of continental lower crust, and provides a quantitative benchmark against which other explanations can be compared.

Received 31 July 2014; accepted 21 January 2016; published online 22 February 2016

References

1. Kelemen, P. B. Genesis of high Mg# andesites and the continental crust. *Contrib. Mineral. Petrol.* **120,** 1–19 (1995).
2. Rudnick, R. L. Making continental crust. *Nature* **378,** 571–577 (1995).
3. Taylor, S. R. The origin and growth of continents. *Tectonophysics.* **4,** 17–34 (1967).
4. Taylor, S. R. & McLennan, S. M. *The Continental Crust: Its Composition and Evolution* (Blackwell, 1985).
5. Taylor, S. R. & McLennan, S. M. The geochemical evolution of the continental crust. *Rev. Geophys.* **33,** 241–265 (1995).
6. Kelemen, P. B., Hanghøj, K. & Greene, A. in *Treatise on Geochemistry* Vol. 3 (ed. Rudnick, R. L.) 593–659 (Elsevier-Pergamon, 2003).
7. Kelemen, P. B., Hanghøj, K. & Greene, A. in *Treatise on Geochemistry* 2nd edn, Vol. 4 (ed. Rudnick, R. L.) 746–805 (Elsevier-Pergamon, 2014).
8. Holbrook, W. S., Mooney, W. D. & Christensen, N. I. in *Continental Lower Crust* (eds Fountain, D. M., Arculus, R. & Kay, R. W.) 1–42 (Elsevier, 1992).
9. Laske, G., Masters, G. & Reif, C. *CRUST2.0: A New Global Crustal Model at 2 × 2 Degrees* http://igppweb.ucsd.edu/~gabi/crust2.html (2001).
10. Christensen, N. I. & Mooney, W. D. Seismic velocity structure and composition of the continental crust; a global view. *J. Geophys. Res. B* **100,** 9761–9788 (1995).
11. Rudnick, R. L. & Fountain, D. M. Nature and composition of the continental crust: a lower crustal perspective. *Rev. Geophys.* **33,** 267–309 (1995).
12. Hacker, B. R., Kelemen, P. B. & Behn, M. D. Continental lower crust. *Annu. Rev. Earth Planet. Sci.* **43,** 167–205 (2015).
13. Rudnick, R. L. & Gao, S. in *Treatise on Geochemistry* Vol. 3 (ed. Rudnick, R. L.) 1–64 (Elsevier-Pergamon, 2003).
14. Rudnick, R. L. & Gao, S. in *Treatise on Geochemistry* 2nd edn, Vol. 4 (ed. Rudnick, R. L.) 1–51 (Elsevier-Pergamon, 2014).
15. Rudnick, R. L. & Presper, T. in *Granulites and Crustal Evolution* (eds Vielzeuf, D. & Vidal, P.) 523–550 (Kluwer, 1990).
16. Huang, Y., Chunakov, V., Mantovani, F., Rudnick, R. L. & McDonough, W. F. A reference Earth model for the heat-producing elements and associated geoneutrino flux. *G-cubed* **14,** 2003–2029 (2013).
17. Behn, M. D. & Kelemen, P. B. Relationship between seismic P-wave velocity and the composition of anhydrous igneous and meta-igneous rocks. *Geochem. Geophys. Geosyst.* **4,** 1041 (2003).
18. Hacker, B. R., Kelemen, P. B. & Behn, M. D. Differentiation of the continental crust by relamination. *Earth Planet. Sci. Lett.* **307,** 501–516 (2011).
19. Kelemen, P. B., Shimizu, N. & Dunn, T. Relative depletion of niobium in some arc magmas and the continental crust: partitioning of K, Nb, La and Ce during melt/rock reaction in the upper mantle. *Earth Planet. Sci. Lett.* **120,** 111–134 (1993).
20. Hacker, B. R. H_2O subduction beyond arcs. *G-cubed* **9,** Q03001 (2008).
21. Jagoutz, O. & Schmidt, M. W. The formation and bulk composition of modern juvenile continental crust: the Kohistan arc. *Chem. Geol.* **298–299,** 79–96 (2012).
22. DeBari, S. M. & Sleep, N. H. High-Mg, low-Al bulk composition of the Talkeetna island arc, Alaska: implications for primary magmas and the nature of arc crust. *Geol. Soc. Am. Bull.* **103,** 37–47 (1991).
23. Greene, A., DeBari, S. M., Kelemen, P. B., Blusztajn, J. & Clift, P. D. A detailed geochemical study of island arc crust: the Talkeetna arc section, south-central Alaska. *J. Petrol.* **47,** 1051–1093 (2006).
24. Jagoutz, O. & Kelemen, P. B. Role of arc processes in the formation of continental crust. *Annu. Rev. Earth Planet. Sci.* **43,** 363–404 (2015).
25. Gill, J. B. *Orogenic Andesites and Plate Tectonics* (Springer, 1981).

26. Grove, T. L. *et al.* Fractional crystallization and mantle-melting controls on calc-alkaline differentiation trends. *Contrib. Mineral. Petrol.* **145,** 515–533 (2003).
27. Blatter, D. L., Sisson, T. W. & Hankins, W. B. Crystallization of oxidized, moderately hydrous arc basalt at mid to lower crustal pressures: implications for andesite genesis. *Contrib. Mineral. Petrol.* **166,** 861–886 (2013).
28. Yogodzinski, G. M., Volynets, O. N., Koloskov, A. V., Seliverstov, N. I. & Matvenkov, V. V. Magnesian andesites and the subduction component in a strongly calc-alkaline series at Piip Volcano, Far Western Aleutians. *J. Petrol.* **35,** 163–204 (1994).
29. Müntener, O., Kelemen, P. B. & Grove, T. L. The role of H_2O during crystallization of primitive arc magmas under uppermost mantle conditions and genesis of igneous pyroxenites: an experimental study. *Contrib. Mineral. Petrol.* **141,** 643–658 (2001).
30. Anderson, A. T. Magma mixing: petrological processes and volcanological tool. *J. Volc. Geotherm. Res.* **1,** 3–33 (1976).
31. Sisson, T. W., Grove, T. L. & Coleman, D. S. Hornblende gabbro sill complex at Onion Valley, California, and a mixing origin for the Sierra Nevada batholith. *Contrib. Mineral. Petrol.* **126,** 81–108 (1996).
32. Shen, B., Jacobsen, B., Lee, C.-T., Yin, Q.-Z. & Morton, D. The Mg isotopic systematics of granitoids in continental arcs and implications for the role of chemical weathering in crust formation. *Proc. Natl Acad. Sci. USA* **106,** 20653 (2009).
33. Albarede, F. & Michard, A. Transfer of continental Mg, S, O, and U to the mantle through hydrothermal alteration of the oceanic crust. *Chem. Geol.* **57,** 1–15 (1986).
34. Rosing, M. T., Bird, D. K., Sleep, N. H., Glassley, W. & Albarede, F. The rise of continents: an essay on the geologic consequences of photosynthesis. *Palaeogeogr. Palaeoclimatol. Palaeoecol.* **232,** 99–113 (2006).
35. Jagoutz, O. Were ancient granitoid compositions influenced by contemporaneous atmospheric and hydrosphere oxidation states? *Terra Nova* **25,** 95–101 (2013).
36. Weaver, B. L. & Tarney, J. Empirical approach to estimating the composition of the continental crust. *Nature* **310,** 575–577 (1984).
37. Cai, Y., Rioux, M. E., Kelemen, P. B., Goldstein, S. L. & Bolge, L. Distinctly different parental magmas for calc-alkaline plutons and tholeiitic lavas in the central and eastern Aleutian arc. *Earth Planet. Sci. Lett.* **431,** 119–126 (2015).
38. Kay, S. M., Kay, R. W. & Perfit, M. R. in *Plutonism from Antarctica to Alaska.* Geological Society of America Special Paper 241 (eds Kay, S. M. & Rapela, C. W.) 233–255 (Geol. Soc. Am., 1990).
39. Kelemen, P. B., Yogodzinski, G. M. & Scholl, D. W. in *Inside the Subduction Factory.* AGU Monograph 138 (ed. Eiler, J.) 293–311 (AGU, 2003).
40. Plank, T. Constraints from thorium/lanthanum on sediment recycling at subduction zones and the evolution of the continents. *J. Petrol.* **46,** 921–944 (2005).
41. Tang, M., Rudnick, R. L., McDonough, W. F., Gaschnig, R. M. & Huang, Y. Europium anomalies constrain the mass of recycled lower continental crust. *Geology* **43,** 703–706 (2015).
42. Behn, M. D., Kelemen, P. B., Hirth, G., Hacker, B. R. & Massonne, H. J. Diapirs as the source of the sediment signature in arc lavas. *Nature Geosci.* **4,** 641–646 (2011).
43. Jull, M. & Kelemen, P. B. On the conditions for lower crustal convective instability. *J. Geophys. Res.* **106,** 6423–6446 (2001).
44. Miller, N. C. & Behn, M. D. Timescales for the growth of sediment diapirs in subduction zones. *Geophys. J. Int.* **190,** 1361–1377 (2012).
45. Ringwood, A. E. & Green, D. H. An experimental investigation of the gabbro-eclogite transformation and some geophysical implications. *Tectonophysics.* **3,** 383–427 (1966).
46. Kay, R. W. & Kay, S. M. Creation and destruction of lower continental crust. *Geol. Rundsch.* **80,** 259–278 (1991).
47. Herzberg, C. T., Fyfe, W. S. & Carr, M. J. Density constraints on the formation of the continental Moho and crust. *Contrib. Mineral. Petrol.* **84,** 1–5 (1983).
48. Ringwood, A. E. The petrological evolution of island arc systems. *J. Geol. Soc. Lond.* **130,** 183–204 (1974).
49. Currie, C. A., Beaumont, C. & Huismans, R. S. The fate of subducted sediments: A case for backarc intrusion and underplating. *Geology* **35,** 1111–1114 (2007).
50. Whitney, D. L., Teyssier, C. & Rey, P. F. The consequences of crustal melting in continental subduction. *Lithosphere* **1,** 323–327 (2009).
51. Behn, M. D. & Kelemen, P. B. Stability of arc lower crust: insights from the Talkeetna arc section, south central Alaska, and the seismic structure of modern arcs. *J. Geophys. Res.* **111,** B11207 (2006).
52. Jagoutz, O. & Schmidt, M. W. The composition of the foundered complement to the continental crust and a re-evaluation of fluxes in arcs. *Earth Planet. Sci. Lett.* **371–372,** 177–190 (2013).
53. Ducea, M. N. & Saleeby, J. B. Buoyancy sources for a large, unrooted mountain range, the Sierra Nevada, California: evidence from xenolith thermobarometry. *J. Geophys. Res.* **101,** 8229–8244 (1996).
54. Wernicke, B. *et al.* Origin of high mountains in the continents: the southern Sierra Nevada. *Science* **271,** 190–193 (1996).
55. Walsh, E. O. & Hacker, B. R. The fate of subducted continental margins: two-stage exhumation of the high-pressure to ultrahigh-pressure Western Gneiss complex, Norway. *J. Metamorph. Geol.* **22,** 671–689 (2004).
56. Grove, M., Jacobson, C. E., Barth, A. P. & Vucic, A. Temporal and spatial trends of Late Cretaceous–early Tertiary underplating of Pelona and related schist beneath southern California and southwestern Arizona. *Spec. Pap. Geol. Soc. Am.* **374,** 381–406 (2003).
57. Bassett, D. *et al.* Three-dimensional velocity structure of the northern Hikurangi margin, Raukumara, New Zealand: implications for the growth of continental crust by subduction erosion and tectonic underplating. *G-cubed* **11,** Q10013 (2010).
58. Scherwath, M. *et al.* Fore-arc deformation and underplating at the northern Hikurangi margin, New Zealand. *J. Geophys. Res.* **115,** B06408 (2010).
59. Enami, M., Mizukami, T. & Yokoyama, K. Metamorphic evolution of garnet-bearing ultramafic rocks from the Gongen area, Sanbagawa belt, Japan. *J. Metamorphic Geol.* **22,** 1–15 (2004).
60. Warren, C. J., Beaumont, C. & Jamieson, R. A. Modelling tectonic styles and ultrahigh pressure (UHP) rock exhumation during the transition from oceanic subduction to continental collision. *Earth Planet. Sci. Lett.* **267,** 129–145 (2008).
61. Sharp, Z. D., Essene, E. J. & Smyth, J. R. Ultra-high temperatures from oxygen isotope thermometry of a coesite-sanidine grospydite. *Contrib. Mineral. Petrol.* **112,** 358–370 (1992).
62. Compagnoni, R. & Maffeo, B. Jadeite-bearing metagranites l.s. and related rocks in the Mount Mucrone area (Sesia-Lanzo Zone, western Italian Alps). *Schweiz. Mineral. Petrogr. Mitt.* **53,** 355–377 (1973).
63. Clift, P. D. & Vannucchi, P. Controls on tectonic accretion versus erosion in subduction zones: Implications for the origin and recycling of the continental crust. *Rev. Geophys.* **42,** 2003RG000127 (2004).
64. Scholl, D. W. & von Huene, R. in *4D Framework of Continental Crust.* Geological Society of America Memoir 200 (eds Robert, J. *et al.*) 9–32 (Geol. Soc. Am., 2007).
65. Ustaszewski, K. *et al.* Crust–mantle boundaries in the Taiwan–Luzon arc-continent collision system determined from local earthquake tomography and 1D models: implications for the mode of subduction polarity reversal. *Tectonophysics* **578,** 31–49 (2012).
66. Arai, R., Iwasaki, T., Sato, H., Abe, S. & Hirata, N. Collision and subduction structure of the Izu–Bonin arc, central Japan, revealed by refraction/wide-angle reflection analysis. *Tectonophysics* **475,** 438–453 (2009).
67. Tetreault, J. L. & Buiter, S. J. H. Geodynamic models of terrane accretion: Testing the fate of island arcs, oceanic plateaus, and continental fragments in subduction zones. *J. Geophys. Res.* **117,** B08403 (2012).
68. Yamamoto, S., Nakajima, J., Hasegawa, A. & Maruyama, S. Izu–Bonin arc subduction under the Honshu island, Japan: evidence from geological and seismological aspect. *Gondwana Res.* **16,** 572–580 (2009).
69. Yamamoto, S., Senshu, H., Rino, S., Omori, S. & Maruyama, S. Granite subduction: arc subduction, tectonic erosion and sediment subduction. *Gondwana Res.* **15,** 443–453 (2009).
70. Plank, T. in *Treatise on Geochemistry* 2nd edn, Vol. 4 (ed. Rudnick, R. L.) 607–629 (Elsevier-Pergamon, 2014).
71. Peterson, B. T. & DePaolo, D. J. Mass and composition of the continental crust estimated using the CRUST2.0 model. *AGU Fall Meeting Abstr.* **1,** 1161 (2007).
72. Holbrook, S. W., Lizarralde, D., McGeary, S., Bangs, N. & Diebold, J. Structure and composition of the Aleutian island arc and implications for continental crustal growth. *Geology* **27,** 31–34 (1999).
73. Fliedner, M. & Klemperer, S. L. Structure of an island arc: wide-angle seismic studies in the eastern Aleutian Islands, Alaska. *J. Geophys. Res.* **104,** 10667–610694 (1999).
74. Shillington, D. J., Van Avendonk, H. J. A., Holbrook, W. S., Kelemen, P. B. & Hornbach, M. J. Composition and structure of the central Aleutian island arc from arc-parallel wide-angle seismic data. *Geochem. Geophys. Geosyst.* **5,** Q10006 (2004).
75. Connolly, J. A. D. Computation of phase equilibria by linear programming: a tool for geodynamic modeling and its application to subduction zone decarbonation. *Earth Planet. Sci. Lett.* **236,** 524–541 (2005).
76. Connolly, J. A. D. Multivariable phase diagrams: an algorithm based on generalized thermodynamics. *Am. J. Sci.* **290,** 666–718 (1990).
77. Ringwood, A. E. Chemical evolution of the terrestrial planets. *Geochim. Cosmochim. Acta* **30,** 41–104 (1966).
78. Barth, M. G., McDonough, W. F. & Rudnick, R. L. Tracking the budget of Nb and Ta in the continental crust. *Chem. Geol.* **165,** 197–213 (2000).
79. Jordan, E. K. *et al. Integrated Earth Data Applications. CentAm & IBM Geochem Database* Version 1.02 (2012); http://dx.doi.org/10.1594/IEDA/100053
80. Hopkins, M. D., Harrison, T. M. & Manning, C. E. Constraints on Hadean geodynamics from mineral inclusions in >4 Ga zircons. *Earth Planet. Sci. Lett.* **298,** 367–376 (2010).

81. Grimes, C. B. *et al.* Trace element chemistry of zircons from oceanic crust: a method for distinguishing detrital zircon provenance. *Geology* **35,** 643–646 (2007).
82. Clift, P. D., Vannucchi, P. & Phipps Morgan, J. Crustal redistribution, crust-mantle recycling and Phanerozoic evolution of the continental crust. *Earth Sci. Rev.* **97,** 80–104 (2009).
83. Hacker, B. R. *et al.* Reconstruction of the Talkeetna intraoceanic arc of Alaska through thermobarometry. *J. Geophys. Res.* **113,** B03204 (2008).
84. Singer, B. S. *et al.* Along-strike trace element and isotopic variation in Aleutian Island arc basalt: subduction melts sediments and dehydrates serpentine. *J. Geophys. Res.* **112,** B06206 (2007).
85. Yogodzinski, G. M. *et al.* The role of subducted basalt in the source of island arc magmas: evidence from seafloor lavas of the western Aleutians. *J. Petrol.* **56,** 441–492 (2015).
86. Jagoutz, O. & Behn, M. D. Foundering of lower arc crust as an explanation for the origin of the continental Moho. *Nature* **504,** 131–134 (2013).

Acknowledgements
We thank B. Hacker and O. Jagoutz for input and inspiration. This paper benefited from suggestions from C. Chauvel. The work was supported by NSF Research Grants EAR 13-16333 (M.D.B.), OCE 11-44759 (P.B.K.) and OCE 13-58091 (P.B.K.).

Author contributions
P.B.K. formulated the hypothesis and compiled geochemical data. M.D.B. performed Perple_X calculations of density for metamorphic xenolith, massif and arc samples. P.B.K. wrote the text and prepared the figures.

Additional information
Supplementary information is available in the online version of the paper. Reprints and permissions information is available online at www.nature.com/reprints. Correspondence should be addressed to P.B.K. or M.D.B.

nature geoscience | SUPPLEMENTARY INFORMATION
DOI: 10.1038/NGEO2662

Formation of lower continental crust by relamination of buoyant arc lavas and plutons

Peter B. Kelemen[1] and Mark D. Behn[2]

1: Dept. of Earth & Environmental Sciences, Columbia University, LDEO, Palisades, NY 10964, peterk@LDEO.columbia.edu
2: Dept. of Geology & Geophysics, WHOI, Woods Hole, MA 02543, mbehn@whoi.edu

Supplementary text

Methods

Calculation of trace element contents of Aleutian and IBM lower crust

Aleutian and IBM lower crust compositions were estimated as follows. Major elements were assumed to be the same as (1,2) major elements in Talkeetna lower crust (from composition 2a in [1]) and (3,4) major elements in Kohistan lower crust (average of three estimates in [2]). Trace elements in log normal average lava and pluton compositions in the Aleutians [3-7] were multiplied by "distribution coefficients" from the following ratios of log normal average values: (1) (Talkeetna lower crust)/(Talkeetna lava) [5,6], (2) (Talkeetna lower crust)/(Talkeetna plutons) [5,6], (3) (Kohistan lower crust)/(Kohistan lava) [2], and (4) (Kohistan lower crust)/(Kohistan plutons) [2]. Izu-Bonin-Mariana (IBM) lower crust compositions were estimated using major elements estimated for IBM lower crust [8], and trace elements calculated as for the Aleutians, using the log normal average of IBM lavas [9] multiplied by (5) (Talkeetna lower crust)/(Talkeetna lava) and (6) (Kohistan lower crust)/(Kohistan lava). See Tables S1 and S4 for all of the values used in these calculations.

Calculation of mineral proportions and densities in different rock compositions

Densities and mineral modes for lavas and plutonic rocks were calculated using Perple_X 6.6.7 [10] with thermodynamic data and solution models appropriate for subduction zone mineral assemblages [11,12]. We assumed 0.5 wt% H_2O in all calculations and set $Fe^{3+}/\Sigma Fe = 0.25$ based on the value found in melt inclusions from Agrigan volcano in the Mariana arc, which is approximately equivalent to ΔQFM+1.5 at 700°C and 3 GPa [13,14]. Densities were calculated for 152 lower crust, 136 mid-crustal pluton and 136 lava samples from the Talkeetna arc [5,6]; 177 lower crust, 86 mid-crustal batholith and 161 lava samples from the Kohistan arc [2]; 1878 lava and 203 plutonic compositions from the Aleutians [3,4,7]; 1440 IBM lavas [9]; and fertile mantle peridotite (pyrolite, [15]), all at 3 GPa and 700°C.

Composition and isotopic evolution of dense residues

In addition to reporting buoyant arc compositions, Table S3 shows the log-normal average composition of dense lithologies from the Talkeetna and Kohistan arcs, where lower crustal rock compositions are known. The dense fractions resemble incompatible-element-depleted, primitive basalts and gabbros.

Although there is previous work on this topic [16,17], we hesitate to draw conclusions about the isotopic evolution of the average composition of this dense component, because individual lithologies (ultramafic cumulates (SiO_2-poor rocks lacking plagioclase feldspar), gabbroic rocks, dense lavas) are likely to form sizeable reservoirs with distinct geochemical characteristics. In three of four compositions, Rb/Sr, U/Pb and Th/Pb in the dense fraction are substantially lower than in the primitive mantle, while Sm/Nd and Lu/Hf parent/daughter ratios are variable and generally close to primitive mantle values.

Uncertainties

Uncertainties in average compositions of lavas and plutons

In various drafts of this paper, we experimented with the use of linear average, median, and log normal average trace element concentrations, where the log normal average is (exp(average(ln(values))). None of the conclusions presented in the paper depend on these choices. In addition to log normal average values, Supplementary Tables 1, 2 and 4 provide linear averages, linear standard deviations, and median values for all of the data sets used in this paper.

We settled on the use of log normal values in the figures and the text because logarithmic histograms of the data look relatively symmetrical about a maximum close to the log normal average (Figures 2, 4, S2 and S7), whereas linear histograms appear skewed toward high values. Thus, the log normal average value provides a better indication of which concentration ranges are most abundant in the various data sets. In a truly representative set of samples from, e.g., continental lower crust, the linear average would provide a better value for the actual lower crust bulk composition, since extremely high concentrations in a few localities can raise the true bulk concentration. However, we are not confident that continental metamorphic xenoliths and massifs comprise a representative set of samples from continental lower crust.

Of more concern are systematic biases in the data. The log-normal average compositions used in this paper represent potentially aliased values, influenced by the varied, specific interests of a host of investigators who sampled and studied continental crust, the Aleutian and IBM arcs, and the Talkeetna and Kohistan arc sections. Uncertainty in the composition of bulk continental crust has endured for decades, and we doubt it will be resolved in the near future. Thus, we use the full range of published estimates to evaluate our hypothesis. In contrast, the average lava compositions used here are fairly robust as a result of extensive, recent studies of Holocene volcanism in the Aleutian and Izu-Bonin-Mariana arcs, and of the Kohistan and Talkeetna crustal sections. Sampling and analysis of the many plutons exposed in the oceanic Aleutian arc has been limited, and resulting averages are uncertain. This is an excellent topic for productive, future research. The nature of a proposed mid-crustal layer of relatively SiO_2-rich plutonic rocks of andesitic composition in the Izu-Bonin-Mariana arc remains uncertain. Perhaps, planned IODP drilling of the arc will provide direct observations of mid-crustal plutons within the arc.

Discussion of Ta and Hf analyses

Hf and Ta analyses (highlighted in Figures 2 and 4) are sometimes subject to systematic error. Ta could be contaminated in analyses of samples prepared by grinding in tungsten carbide vessels. None of the Kohistan or Talkeetna lower crust analyses published in this century were done on powders ground in tungsten carbide. We did not check the analytical methods used for the thousands of metamorphic rock samples used to estimate lower continental crust compositions, nor for the thousands of Aleutian and IBM arc lava compositions we used. However, one might expect Ta contamination to be most significant in samples with low Ta concentration, raising the apparent concentration in those samples. In contrast, a central point in our paper is that arc lower crust Ta concentrations are significantly *lower* than estimated lower continental crust. If a significant number of Ta-depleted arc samples were contaminated, then the actual Ta concentration in the depleted samples is yet lower, leaving our conclusion unchanged.

Similarly, Hf in some ICP-MS analyses is too low because of incomplete digestion of zircon when samples were dissolved. When working on the Talkeetna arc, we were careful to compare XRF and ICP-MS analyses of Zr to ensure that any zircon present in the samples was fully dissolved. (Indeed, we searched for zircon for U/Pb geochronology, but could not extract any zircon out of most Talkeetna lower crust samples). XRF and ICP-MS analyses were also compared for Kohistan arc lower crust. Thus, the low Zr concentration samples in arc lower crust are well analyzed. This said, we did not check the thousands of other compositions used in this paper.

One might expect zircon to be most abundant in relatively SiO_2-rich samples with high incompatible trace element concentrations, such as in felsic granulites that are important constituents of estimated lower continental crust compositions. In contrast, a central point in our paper is that estimates for lower continental crust have significantly higher Hf concentrations than arc lower crust. If the analyses of trace element rich compositions used to construct estimates for lower continental crust were missing Hf in undissolved zircon, then the actual Hf concentrations in these samples would be even higher, again leaving our conclusion unchanged.

Uncertainties in estimates of lower crust and bulk crust compositions

Our estimates of Aleutian and Izu-Bonin-Mariana lower crust compositions are uncertain. Table S1 presents the data and assumptions used to make these estimates in spreadsheet form, and readers are encouraged to experiment with this spreadsheet to determine the sensitivity of particular results to the choice of input parameters.

However, the following overall results are robust:

(1) Arc lower crust has higher Mg# and lower SiO_2 than average lavas and felsic plutons (Figure S1), and incompatible element concentrations that are less than half – almost certainly, less than one third – of their concentrations in average lavas and plutons (Figures 1, 2, S1 and S3).
(2) Seismic data – where available – indicate that the lower crust comprises more than half of the Aleutian and Izu-Bonin-Mariana arc sections.
(3) *Ta, K, La, Ce and Hf are systematically more depleted in arc lower crust than in samples of LCC*.

As a result, since incompatible element concentrations in average lavas and plutons are less than or equal to concentrations in continental crust, bulk arc crust must be substantially depleted in these elements compared to continental crust, even after proposed delamination processes.

Finally,

(4) lithologies typical of arc lower crust are denser than mantle peridotite under subduction zone conditions at <700°C and 3 to 4 GPa [18-21].

Arc subduction and density sorting would separate buoyant, relatively SiO_2-rich lavas and plutons from SiO_2-poor arc lower crust (Figure S8), adding an incompatible element enriched component to the overlying crust, while the depleted lower crustal lithologies, together with SiO_2-poor lithologies among lavas and plutons, continued to subduct.

Choice of reference pressure and temperature for calculating densities

In separating buoyant and dense compositions, we used a cutoff of 3377 kg/m^3, based on the estimated density of pyrolite [15] at 700°C, 3 GPa. The results were similar for densities calculated at 700°C, 4 GPa, 800°C, 3 GPa, and 800°C, 4 GPa, indicating that the choice of pressure and temperature conditions along a subduction zone geotherm is not a large source of uncertainty in our results.

The effect of density variations due to composition and temperature

Compositions with densities close to pyrolite are close to neutral buoyancy, and would be very slow to form density instabilities [20]. On the other hand, some layered sections, incorporating a small proportion of dense inclusions, but with a significant, positive average buoyancy, are likely to become unstable. Evidence for this is provided by the presence of dense, SiO_2-poor inclusions within buoyant, relatively SiO_2-rich gneisses in UHP metamorphic terrains worldwide.

Heating of subducting upper crust to ~ 700–800°C is predicted to occur over a substantial time and depth interval [22]. Thus, in the simplest possible scenario, one might expect heating and ascent of buoyant mid-crustal plutons at a greater subduction depth than for buoyant volcanic compositions. However, we expect that the natural relamination process involves a series of instabilities, removing hot, buoyant layers from the top of the subducting plate, followed by rapid heating of newly exposed, successively deeper layers in the subducting material. Furthermore, in the process of subduction erosion, arc lavas and plutons are likely to be juxtaposed and mechanically mixed.

Caveats and future work

Recycling of a sediment component is not important in producing arc lavas with compositions in the range of estimated BCC and LCC

While we have summarized the evidence that arc magmatism plays a key role in forming continental crust, an alternative view is that arc magmas resemble continental crust *because* they include a recycled component from subducted, continentally-derived sediments. However, isotope data show that this is not the case. Some arc lavas that lie within the compositional range of estimated BCC and LCC are the most isotopically depleted arc magmas worldwide (Figure S3), with little or no contribution from recycled, older continental material [5,6]. Thus, recycling of subducted sediment is not the cause of the compositions similar to BCC and LCC, at least, not always. Instead, it is evident that juvenile igneous material with a major and trace element composition similar to continental crust is being extracted from the Earth's mantle via arc magmatic processes.

This is clearest for the oceanic Aleutian volcanic arc, extending from Alaska to Russia between the Bering Sea and the Pacific Ocean. Primitive andesites and dacites in the western Aleutians (165°E to 177°W) are the most isotopically depleted arc magmas worldwide (Figure S3), with little or no contribution from recycled, older continental material [5,6]. Exposed plutonic rocks throughout the oceanic arc (west and east) have average major element, trace element and isotopic characteristics similar to western Aleutian lavas [3,23,24]. Lavas from the central Aleutians (177 to 164°W) have isotope ratios indicative of recycling of a terrigenous sediment component (reviews in [5-7]), but the trace element characteristics of the lavas are similar to the western Aleutians (Table S1).

Is some arc crust similar to continental crust, even without density sorting?

It is possible that at some times and places, arc magmatism forms crust similar to continental crust without substantial density sorting. For example, in Costa Rica the composition of young volcanic rocks (<10 Ma) and the lower crustal seismic velocity are very similar to continental crust [25]. On the other hand, it is not clear what happened to the SiO_2-poor arc crust that formed in Costa Rica prior to 10 Ma. Perhaps, it was removed by vigorous subduction erosion in that region [26], after which subducted, buoyant lithologies were relaminated to form some of the current arc lower crust. More generally, global arc magmatism commonly forms abundant basalts and SiO_2-poor crust, with lower SiO_2 and higher lower crustal seismic velocities than continental crust. In these cases, a process such as arc subduction and density sorting is required to separate the components that comprise continental crust.

Modification of relaminating material via reaction with mantle peridotite and anatexis

The buoyant arc compositions calculated in this paper could be modified by a variety of processes during ascent and relamination, and these processes could affect their geophysical characteristics.

Ascending, buoyant diapirs probably react with mantle peridotite, lowering their SiO_2 contents, increasing their MgO and Ni contents, and modifying other major elements in a manner analogous with the inferred genesis of primitive andesites and dacites (reviews in [3,5,6]). Such processes, when they occur at high melt/rock ratios, have little effect on incompatible element concentrations but increase the seismic wave speeds in the resulting, relaminated lithologies.

It is likely that buoyant compositions undergo small degrees of partial melting during ascent and after relamination at the base of the crust, forming an SiO_2-rich melt with high concentrations of incompatible elements including K, Th and U. This melt may often ascend into the upper crust, leaving a K, Th and U depleted residue in the lower crust [27], for example as demonstrated for metamorphic xenoliths from New Mexico [28].

Relamination processes in the early Earth

Several aspects of the process described here may have been different on the early Earth. Low fO_2 might have rendered crystallization of Fe-Ti oxide minerals – to form high Mg# andesites from basalts – less likely. On the other hand, high Mg# andesites and dacites with “enriched” trace-element concentrations may have been more common as the result of extensive partial melting of basaltic lithologies as they subducted or foundered into a hotter mantle (e.g., [29,30]). The mantle wedge above Archean subduction zones may have been composed of highly depleted, residual dunite [31] that reacted with ascending melts but only contributed a small mantle component to arc magmatism compared to modern arcs [32].

Supplementary Figure Captions

Supplementary Figure S1: Compositions of continental crust, mid-ocean ridge basalt, and magmatic rocks in volcanic arcs. **A.** Estimates for the composition of the upper, lower and bulk continental crust (compilations in [33-35]). The red and black polygons in panels A-F enclose all published estimates for bulk continental crust. **B.** Mid-ocean ridge basalts [36-38] follow a low H_2O, low fO_2 crystallization path, beginning with mantle-derived, primitive basalts with Mg#>0.6. This does not produce any compositions similar to continental crust. Abbreviations: EPR: East Pacific Rise; MAR: Mid-Atlantic Ridge; Indian: Indian Ocean ridges; JDF: Juan de Fuca Ridge. **C.** Lavas and plutons from the Aleutian arc [3,4,7], particularly at and west of Adak Island, are the most similar to continental crust of any intra-oceanic arc, worldwide [5,6]. **D.** Lavas from the Izu-Bonin-Mariana arc [9]. **E.** Lower crust, mid-crustal plutons, and lavas from the Talkeetna arc section [5,6]. Bulk crustal estimate is composition 2a in Table 8 of Hacker et al. [1]. **F.** Lower crust, mid-crustal batholith, lavas and bulk crust for the Kohistan arc section [2]. **G.** Extended trace element diagram for average Aleutian lavas (data sources as for panel **C**), Aleutian plutons [3,23], Izu-Bonin-Marianas (IBM) lavas (data as in **D**), mid-ocean ridge basalts (data as in **B**) and estimated BCC (yellow field) and LCC (grey field) (data compilations in [19,33-35,39]), with all values normalized to the BCC composition of Rudnick and Gao [34,35]. **H.** Extended trace element diagram for Aleutian lavas and plutons with high Mg# andesite compositions of 54-65wt% SiO_2, Mg# 0.43-0.55 [33] (data as in **G**). All elements except Nb and Ta in lavas lie within the bounds for estimates of lower continental crust, and are within a factor of two of Rudnick & Gao's estimate for bulk continental crust [34,35]. All elements in high Mg# andesite plutons lie within the bounds for estimates of bulk continental crust. **I.** Extended trace element diagram for average Kohistan lavas and batholith (data as in **F**) and average Talkeetna lavas and plutons (data as in **E**).

Supplementary Figure S2: La, Ce and K in Talkeetna and Kohistan arc lower crust are systematically lower than in LCC as represented by continental metamorphic xenoliths and massifs. Data sources as for Figure 1. See Figure 2 for Hf and Ta concentrations. Compositions of Kohistan ultramafic rocks (SiO_2-poor rocks with no plagioclase feldspar) at depths greater than 55 km are not plotted.

Supplementary Figure S3: Comparison of isotope ratios for western Aleutian lavas (red symbols) compared to all other arc magmas, worldwide [5,6], demonstrating that western Aleutian magmas contain the smallest proportion of material derived from older continental crust via sediment subduction and recycling. (New, more extensive data – not plotted – confirm this [7]). Nevertheless, western Aleutian lavas have major and trace element compositions more similar to continental crust than lavas in any other intra-oceanic arc worldwide [3,5,25]. Thus, magmatic rocks in the western Aleutians represent juvenile crust, and provide an analogue for the initial formation of igneous rocks with the composition of continental crust in the early Earth.

Supplementary Figure S4: A. Experimental crystallization of primitive andesites produces high Mg# andesites and dacites similar to continental crust (Table S2) [21,40]. **B.** Experimental crystallization of primitive basalt and basaltic andesite at high H_2O and fO_2 yields Fe-oxide- and hornblende-bearing solid products, and high Mg# andesites and dacites similar to continental crust [40,41]. Also see Berndt et al. [42] **C.** Mixing of basalt formed by 10% olivine crystallization from global and Aleutian average, primitive lavas [5] with average low Si granite from the Sierra Nevada [43] could produce high Mg# andesites and dacites similar to continental crust.

Supplementary Figure S5: Schematic illustration of three paths for relamination of buoyant, subducted materials, discussed in the text. The inset illustrates the relative efficiency of arc subduction and density sorting (right), versus delamination of garnet-bearing lithologies from the base of arc crust (middle), in removing SiO_2-poor material while retaining relatively SiO_2-rich lithologies similar to continental crust.

Supplementary Figure S6: Calculated density of the average composition of buoyant Aleutian and IBM lavas and plutonic rocks relative to the density of fertile mantle peridotite (pyrolite) along **A.** a hot geotherm (Cascadia) and **B.** a cold geotherm (Marianas) from the thermal models of Wada and Wang [44], using the thermodynamic minimization code Perple_X [10,45] following the methods described in the Supplementary Text. **C.** Calculated mineral proportions in the average Aleutian plutonic rock composition along the Cascadia geotherm. **D.** Instability times as a function of temperature and buoyant layer thickness, calculated for buoyant layers 100 kg/m^3 less dense than the overlying mantle, as described by Behn et al. [46]. Readers can also refer to a similar diagram, Figure 4 in that paper, calculated for a density contrast of 200 kg/m^3.

Supplementary Figure S7: Compositional consequences of subduction and density sorting, for the Aleutian (**A, E**), Izu-Bonin Mariana (**B, F**), Kohistan (**C,G**) and Talkeetna (**D,H**) arcs. In panels **A-D**, the polygon encloses all published estimates for bulk continental crust, and stars indicate the average composition of buoyant lavas (purple) and plutonic rocks (yellow). In panels **E-H**, buoyant lava and pluton compositions from the Aleutians, IBM, Kohistan and Talkeetna arcs, normalized to the bulk continental crust estimate of Rudnick and Gao [34,35], are compared to upper and lower bounds for the composition of bulk continental crust (yellow field) and lower continental crust (grey field). Data sources as for Figure S1.

Supplementary Figure S8: Density sorting efficiently separates incompatible enriched, buoyant samples similar to LCC from incompatible element depleted, dens samples. **(A-D)** Ta, K, La and Hf concentrations versus calculated density at 700°C, 3 GPa, for Talkeetna and Kohistan samples. Samples < 3377 kg/m^3 (density of pyrolite [15]) have Hf and Ta comparable to LCC. **(E,F)** Hf versus Ta and K versus La concentrations for lava and plutonic samples from the Kohistan and Talkeetna arcs with calculated densities < pyrolite at 700°C, 3 GPa, compared to LCC as represented by continental metamorphic xenoliths and terrains [19,47]. Data sources as for Figure 1. Note the striking difference between this plot and Figure 2.

References cited only in Tables

McDonough & Sun [48]

References cited

1 Hacker, B. R. *et al.* Reconstruction of the Talkeetna intraoceanic arc of Alaska through thermobarometry. *J. Geophys. Res.* **113**, doi 10.1029/2007jb005208 (2008).

2 Jagoutz, O. & Schmidt, M. W. The formation and bulk composition of modern juvenile continental crust: The Kohistan arc. *Chem. Geol* **298-299**, 79-96 (2012).

3 Kelemen, P. B., Yogodzinski, G. M. & Scholl, D. W. in *Inside the Subduction Factory, AGU Monograph 138* (ed J. Eiler) 293-311 (American Geophysical Union, 2003).

4 Singer, B. S. *et al.* Along-strike trace element and isotopic variation in Aleutian Island arc basalt: Subduction melts sediments and dehydrates serpentine. *J. Geophys. Res.* **112**, doi:10.1029/2006JB004897 (2007).

5 Kelemen, P. B., Hanghøj, K. & Greene, A. in *The Crust, Vol. 3, Treatise on Geochemistry, (H.D. Holland and K.K. Turekian, eds.)* Vol. 3 (ed Roberta L Rudnick) 593-659 (Elsevier-Pergamon, 2003).

6 Kelemen, P. B., Hanghøj, K. & Greene, A. in *The Crust, Vol. 4, Treatise on Geochemistry, 2nd edition (H.D. Holland and K.K. Turekian, eds.)* (ed Roberta L Rudnick) 746-805 (Elsevier-Pergamon, 2014).

7 Yogodzinski, G. M. *et al.* The role of subducted basalt in the source of island arc magmas: Evidence from seafloor lavas of the western Aleutians. *J. Petrol.* **56**, 441-492 (2015).

8 Tatsumi, Y. *et al.* Structure and growth of the Izu-Bonin-Mariana arc crust: 2. Role of crust-mantle transformation and the transparent Moho in arc crust evolution. *J. Geophys. Res.* **113**, doi:10.1029/2007JB005121 (2008).

9 Jordan, E. K. *et al.* CentAm & IBM Geochem Database version 1.02. *Integrated Earth Data Applications* http://www.iedadata.org/doi?id=100053, doi: 10.1594/IEDA/100053 (2012).

10 Connolly, J. A. D. Computation of phase equilibria by linear programming: A tool for geodynamic modeling and its application to subduction zone decarbonation. *Earth Planet. Sci. Lett.* **236**, 524 -541 (2005).

11 Holland, T. & Powell, R. Activity-composition relations for phases in petrological calculations: An asymmetric multicomponent formulation. *Contrib. Mineral. Petrol.* **145**, 492-501 (2003).

12 Hacker, B. R. H2O subduction beyond arcs. *G-cubed* **9**, doi:10.1029/2007GC001707 (2008).

13 Kelley, K. A. & Cottrell, E. The influence of magmatic differentiation on the oxidation state of Fe in a basaltic arc magma. *Earth Planet. Sci, Lett,* **329-330**, 109-121 (2012).

14 Kress, V. C. & Carmichael, I. S. E. The compressibility of silicate liquids containing Fe2O3 and the effect of composition, temperature, oxygen fugacity and pressure on their redox states. *Contrib. Mineral. Petrol.* **108**, 82-92 (1991).

15 Ringwood, A. E. Chemical evolution of the terrestrial planets. *Geochim. Cosmochim. Acta* **30**, 41-104 (1966).

16 Jagoutz, O. & Schmidt, M. W. The composition of the foundered complement to the continental crust and a re-evaluation of fluxes in arcs. *Earth Planet. Sci. Lett.* **371-372**, 177-190 (2013).
17 Tatsumi, Y. Continental crust formation by crustal delamination in subduction zones and complementary accumulation of the enriched mantle I component in the mantle. *G-cubed* **1**, paper number 2000GC000094 (2000).
18 Behn, M. D. & Kelemen, P. B. Stability of arc lower crust: Insights from the Talkeetna arc section, south central Alaska, and the seismic structure of modern arcs. *Journal of Geophysical Research-Solid Earth* **111**, doi:10.1029/2006jb004327 (2006).
19 Hacker, B. R., Kelemen, P. B. & Behn, M. D. Continental lower crust. *Ann. Rev. Earth Planet. Sci.* **43**, 167-205 (2015).
20 Jull, M. & Kelemen, P. B. On the conditions for lower crustal convective instability. *J. Geophys. Res.* **106**, 6423-6446 (2001).
21 Müntener, O., Kelemen, P. B. & Grove, T. L. The role of H2O during crystallization of primitive arc magmas under uppermost mantle conditions and genesis of igneous pyroxenites: An experimental study. *Contrib. Mineral. Petrol.* **141**, 643-658 (2001).
22 Miller, N. C. & Behn, M. D. Timescales for the growth of sediment diapirs in subduction zones. *Geophys. J. Int.* **190**, 1361-1377 (2012).
23 Cai, Y., Rioux, M. E., Kelemen, P. B., Goldstein, S. L. & Bolge, L. Distinctly different parental magmas for calc-alkaline plutons and tholeiitic lavas in the central and eastern Aleutian arc. *Earth Planet. Sci, Lett,* **in press** (2015).
24 Kay, S. M., Kay, R. W. & Perfit, M. R. in *Plutonism from Antarctica to Alaska, Geological Society of America Special Paper* Vol. 241 (eds S. M. Kay & C.W. Rapela) 233-255 (Geol. Soc. Amer., 1990).
25 Gazel, E. *et al.* The youngest continents. *Nature Geosci.* **in revision** (2014).
26 Ranero, C. R. & von Huene, R. Subduction erosion along the Middle America convergent margin. *Nature* **404**, 748-752 (2000).
27 Hacker, B. R., Kelemen, P. B. & Behn, M. D. Differentiation of the continental crust by relamination. *Earth Planet. Sci, Lett,* **307**, 501-516, doi:10.1016/j.epsl.2011.05.024 (2011).
28 Reid, M. R., Hart, S. R., Padovani, E. R. & Wandless, G. A. Contribution of metapelitic sediments to the composition, heat production, and seismic velocity of the lower crust of southern New Mexico, U.S.A. *Earth Planet. Sci, Lett,* **95**, 367-381 (1989).
29 Ringwood, A. E. The petrological evolution of island arc systems. *J. Geol. Soc. Lond.* **130**, 183-204 (1974).
30 Martin, H. Effect of steeper Archean geothermal gradient on geochemistry of subduction-zone magmas. *Geology* **14**, 753-756 (1986).
31 Bernstein, S., Kelemen, P. B. & Hanghøj, K. Consistent olivine Mg# in cratonic mantle reflects Archean mantle melting to the exhaustion of orthopyroxene. *Geology* **35**, 459-462 (2007).
32 Kelemen, P. B., Hart, S. R. & Bernstein, S. Silica enrichment in the continental upper mantle lithosphere via melt/rock reaction. *Earth Planet. Sci. Lett.* **164**, 387-406 (1998).

33 Kelemen, P. B. Genesis of high Mg# andesites and the continental crust. *Contrib. Mineral. Petrol.* **120**, 1-19 (1995).
34 Rudnick, R. L. & Gao, S. in *The Crust, Vol. 4, Treatise on Geochemistry, 2nd edition (H.D. Holland and K.K. Turekian, eds.)* (ed R.L. Rudnick) 1-51 (Elsevier-Pergamon, 2014).
35 Rudnick, R. L. & Gao, S. in *The Crust, Vol. 3, Treatise on Geochemistry (H.D. Holland and K.K. Turekian, eds.)* Vol. 3 (ed R.L. Rudnick) 1-64 (Elsevier-Pergamon, 2003).
36 Su, Y.-J. *Mid-ocean ridge basalt trace element systematics: Constraints from database management, ICP-MS analyses, global data compilation, and petrologic modeling* PhD thesis, Columbia University, (2002).
37 Wanless, V. D., Perfit, M. R., Ridley, W. I. & Klein, E. Dacite petrogenesis on mid-ocean ridges: Evidence for oceanic crustal melting and assimilation. *J. Petrol.* **51**, 2377-2410 (2010).
38 Gale, A., Dalton, C. A., Langmuir, C. H., Su, Y. & Schilling, J.-G. The mean composition of ocean ridge basalts. *G-cubed* **14**, 489-518 (2013).
39 Rudnick, R. L. & Fountain, D. M. Nature and composition of the continental crust: A lower crustal perspective. *Rev. Geophys.* **33**, 267-309 (1995).
40 Grove, T. L. *et al.* Fractional crystallization and mantle-melting controls on calc-alkaline differentiation trends. *Contrib. Mineral. Petrol.* **145**, 515-533 (2003).
41 Blatter, D. L., Sisson, T. W. & Hankins, W. B. Crystallization of oxidized, moderately hydrous arc basalt at mid to lower crustal pressures: Implications for andesite genesis. *Contrib. Mineral. Petrol.* **166**, 861-886 (2013).
42 Berndt, J., Koepke, J. & Holtz, F. An experimental investigation of the influence of water and oxygen fugacity on differentiation of MORB at 200 MPa. *J. Petrol.* **46**, 135-167 (2005).
43 Sisson, T. W., Grove, T. L. & Coleman, D. S. Hornblende gabbro sill complex at Onion Valley, California, and a mixing origin for the Sierra Nevada batholith. *Contrib. Mineral. Petrol.* **126**, 81-108 (1996).
44 Wada, I. & Wang, K. Common depth of slab-mantle decoupling: Reconciling diversity and uniformity of subduction zones. *G-cubed* **10**, doi:10.1029/2009GC002570 (2009).
45 Connolly, J. A. D. Multivariable phase diagrams an algorithm based on generalized thermodynamics. *Am. J. Sci.* **290**, 666-718 (1990).
46 Behn, M. D., Kelemen, P. B., Hirth, G., Hacker, B. R. & Massonne, H. J. Diapirs as the source of the sediment signature in arc lavas. *Nature Geosci.* **4**, 641-646, doi:10.1038/ngeo1214 (2011).
47 Huang, Y., Chunakov, V., Mantovani, F., Rudnick, R. L. & McDonough, W. F. A reference Earth model for the heat-producing elements and associated geoneutrino flux. *G-cubed* **14**, 2003-2029 (2013).
48 McDonough, W. F. & Sun, S.-S. The composition of the Earth. *Chem. Geol.* **120**, 223-253 (1995).

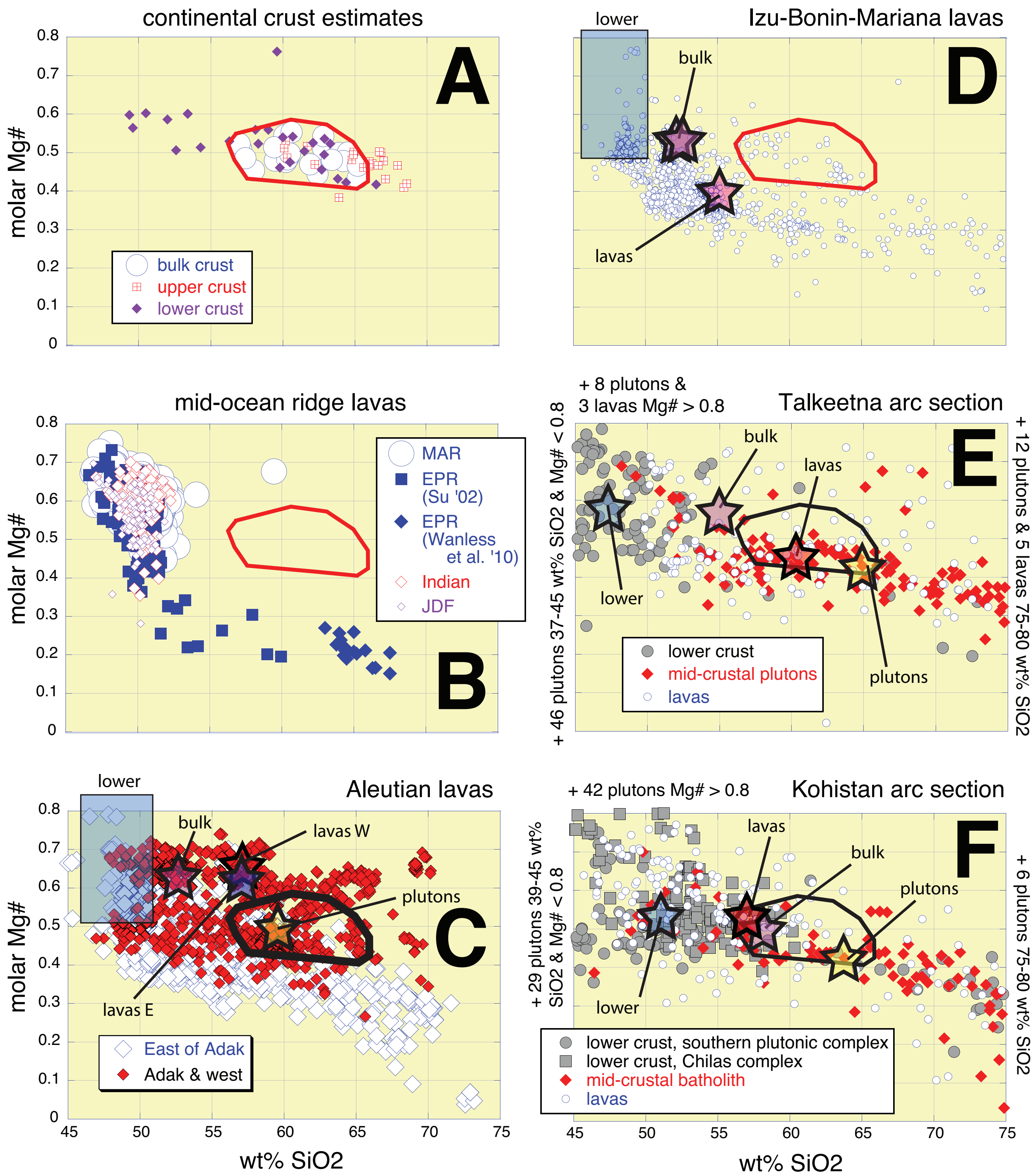

Kelemen & Behn Supplementary Figure S1A-F

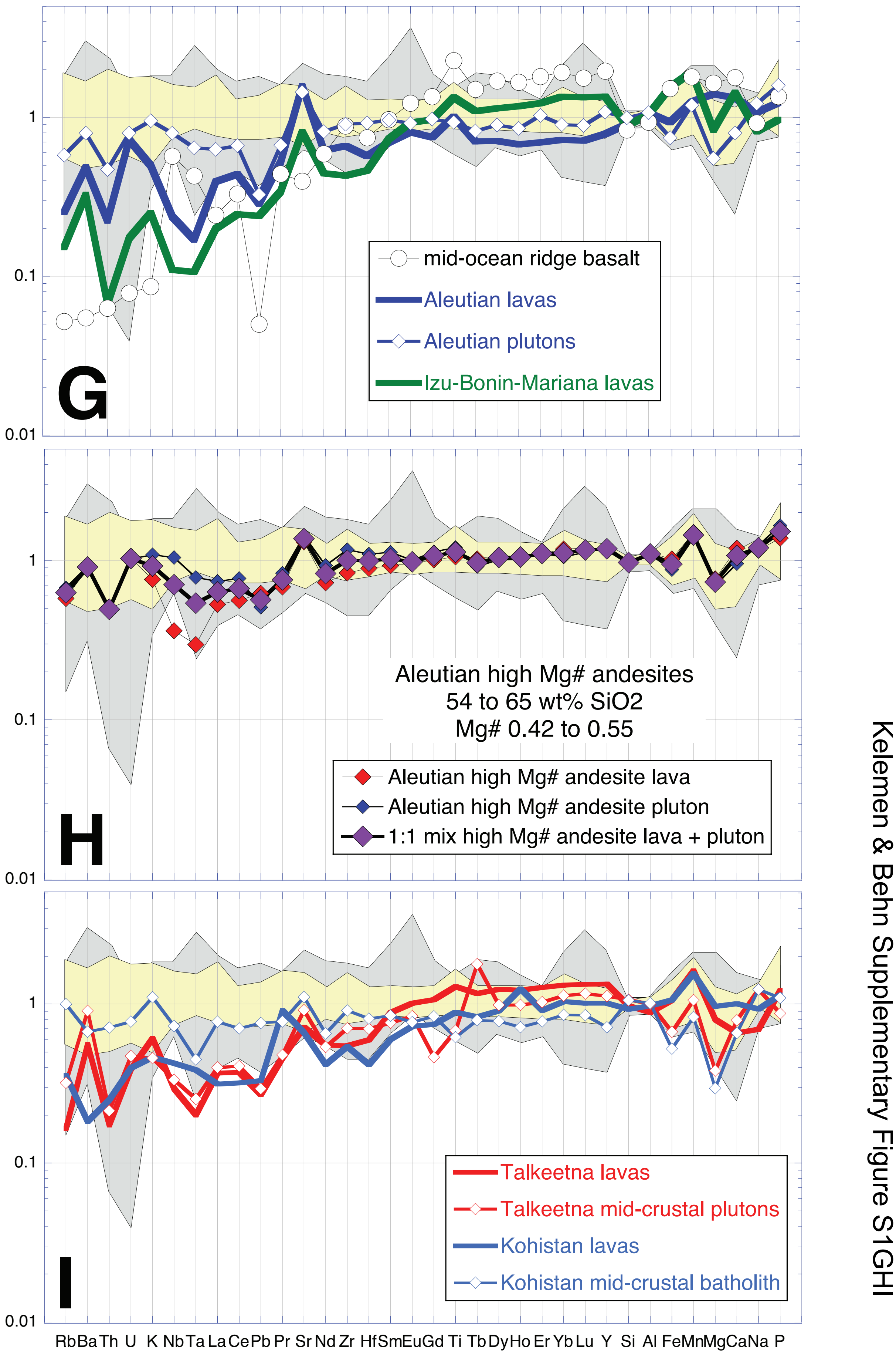
G
mid-ocean ridge basalt
Aleutian lavas
Aleutian plutons
Izu-Bonin-Mariana lavas
H
Aleutian high Mg# andesites
54 to 65 wt% SiO2
Mg# 0.42 to 0.55
Aleutian high Mg# andesite lava
Aleutian high Mg# andesite pluton
1:1 mix high Mg# andesite lava + pluton
I
Talkeetna lavas
Talkeetna mid-crustal plutons
Kohistan lavas
Kohistan mid-crustal batholith
1
0.1
0.01
Rb Ba Th U K Nb Ta La Ce Pb Pr Sr Nd Zr Hf Sm Eu Gd Ti Tb Dy Ho Er Yb Lu Y Si Al Fe Mn Mg Ca Na P
Kelemen & Behn Supplementary Figure S1GHI

Kelemen & Behn Supplementary Figure S2

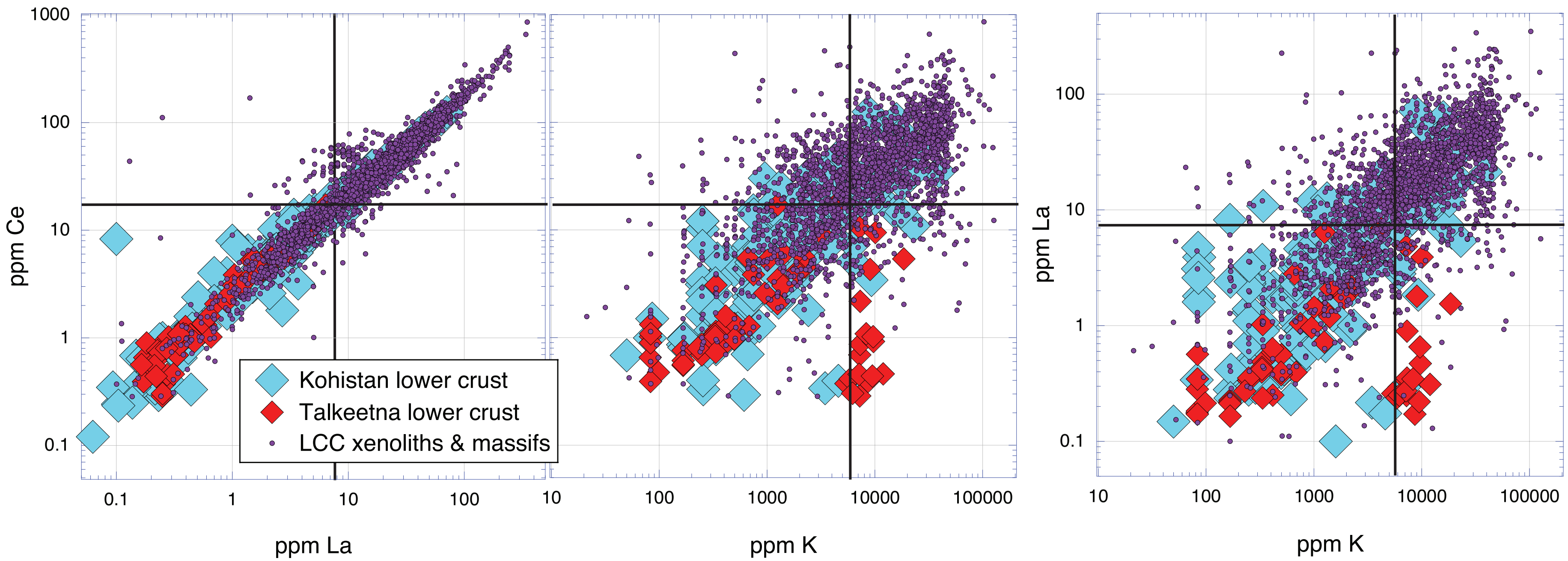

Kelemen & Behn Supplementary Figure S3

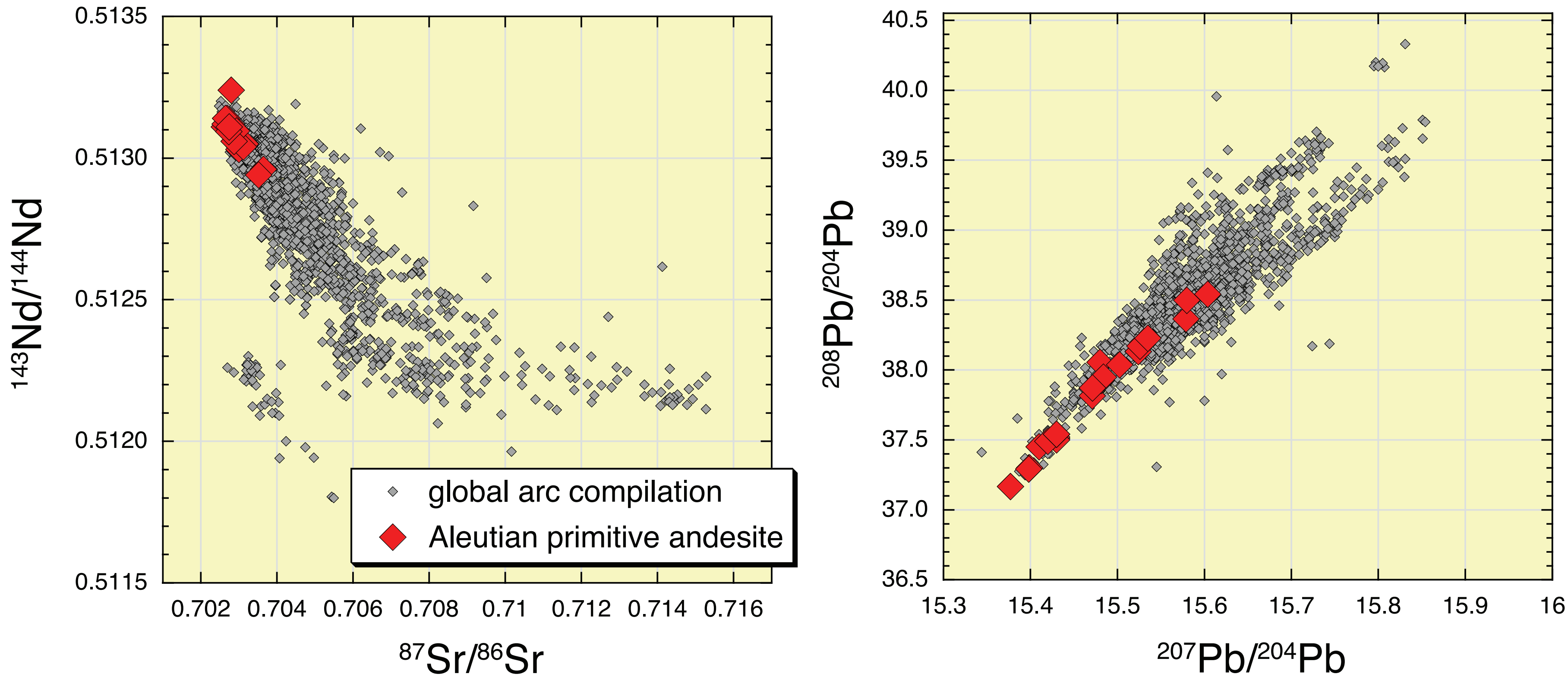

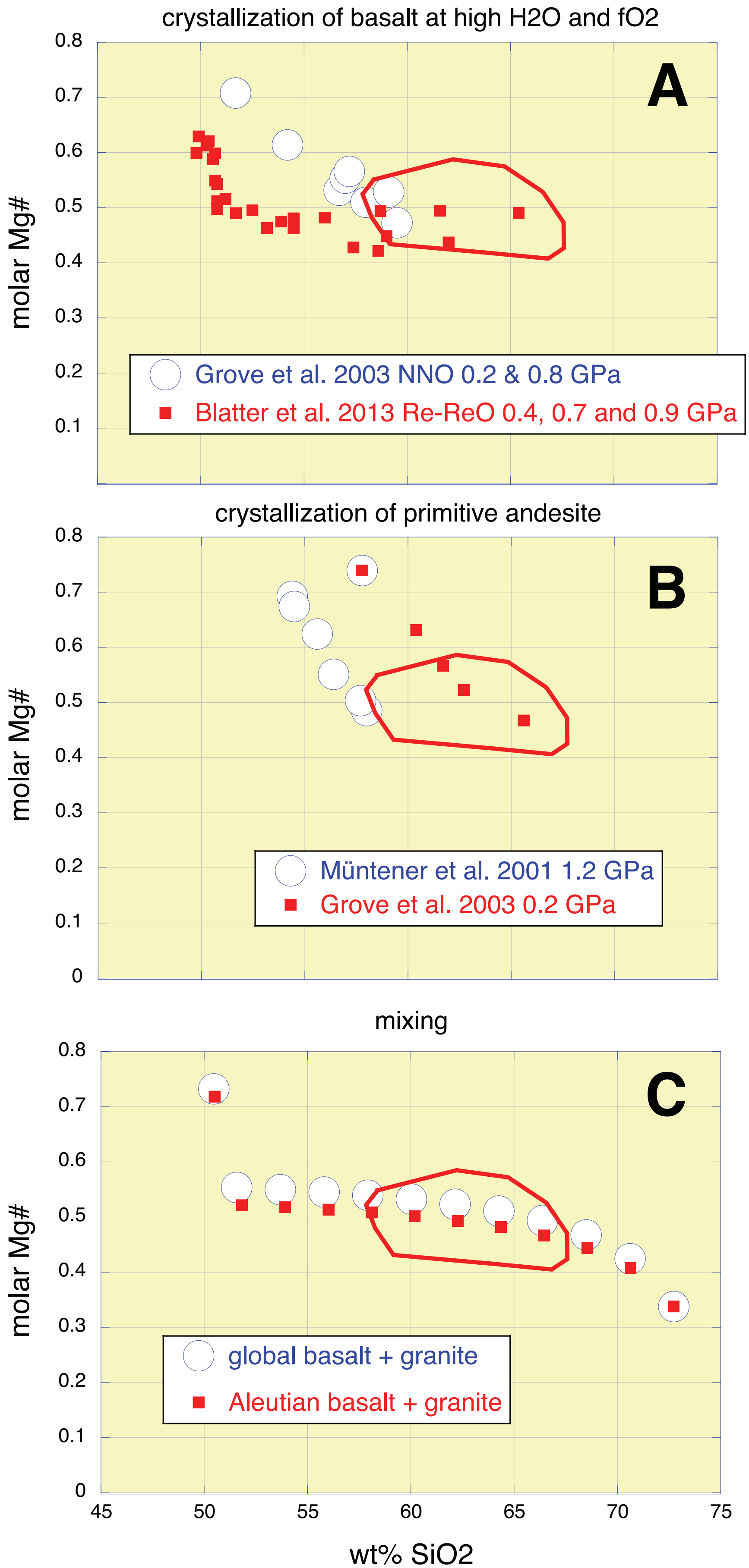

1GHI

Kelemen & Behn Supplementary Figure S4

Kelemen & Behn Supplementary Figure S5

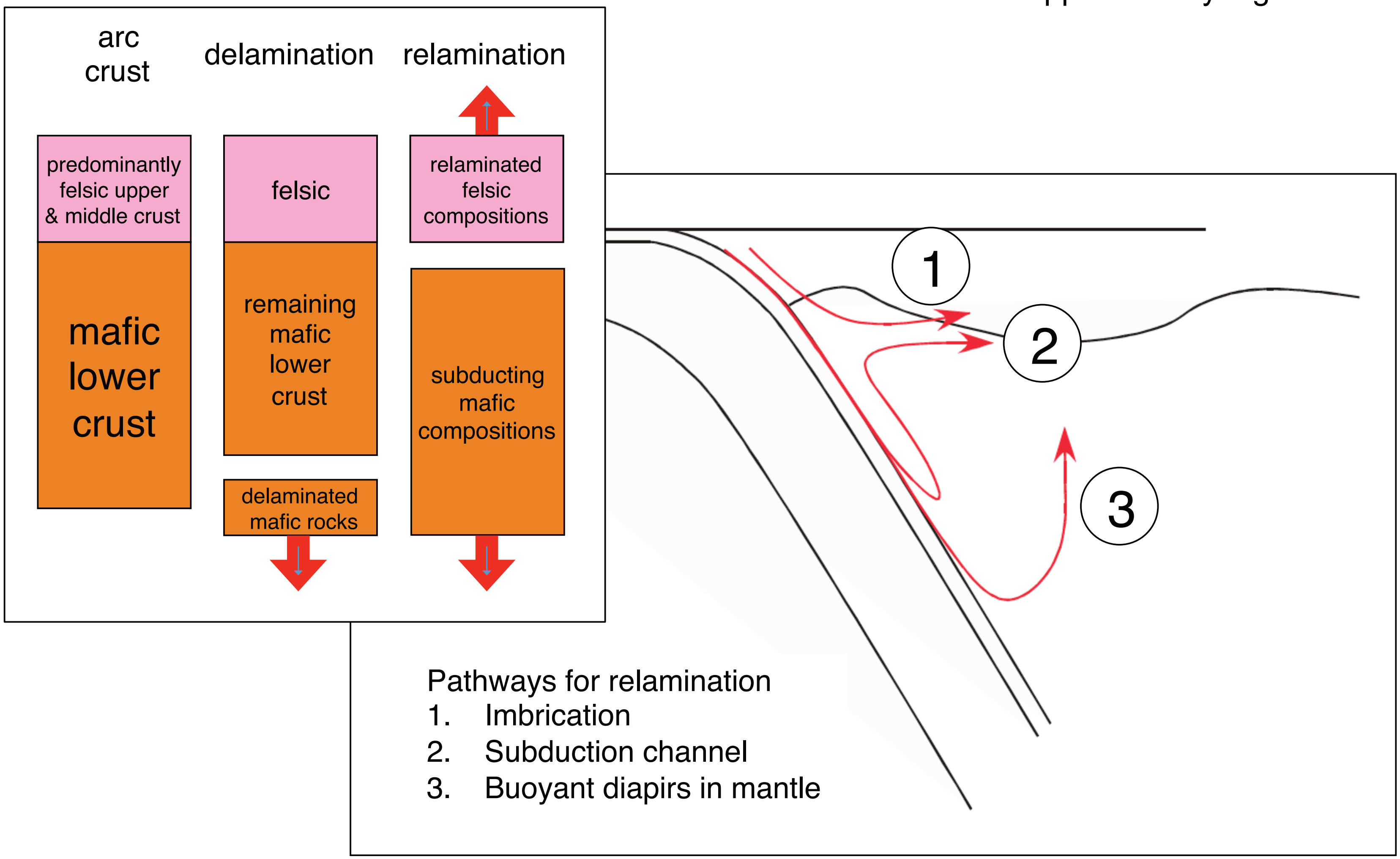

Kelemen & Behn Supplementary Figure S6

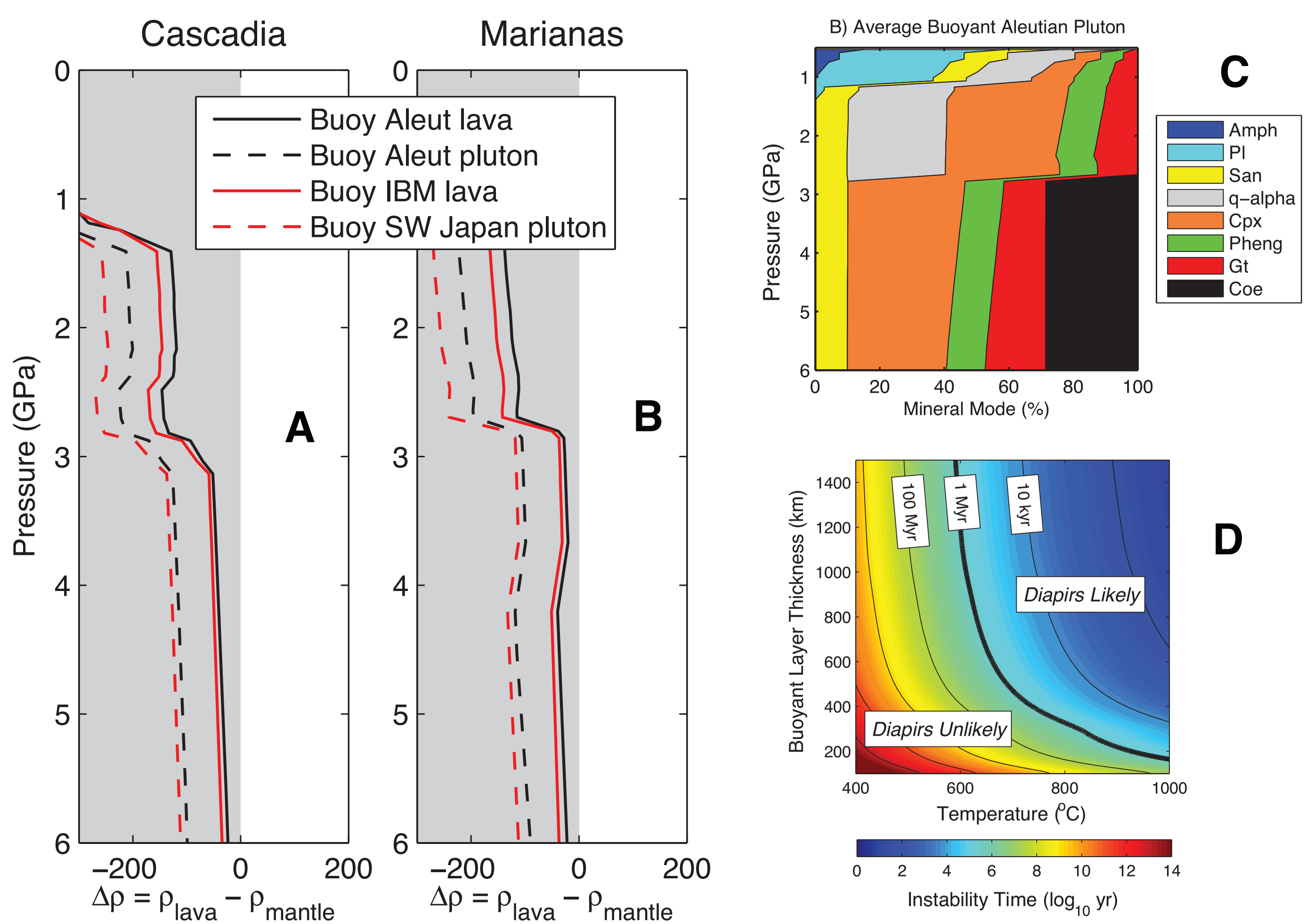

Kelemen & Behn Supplementary Figure S7A-D

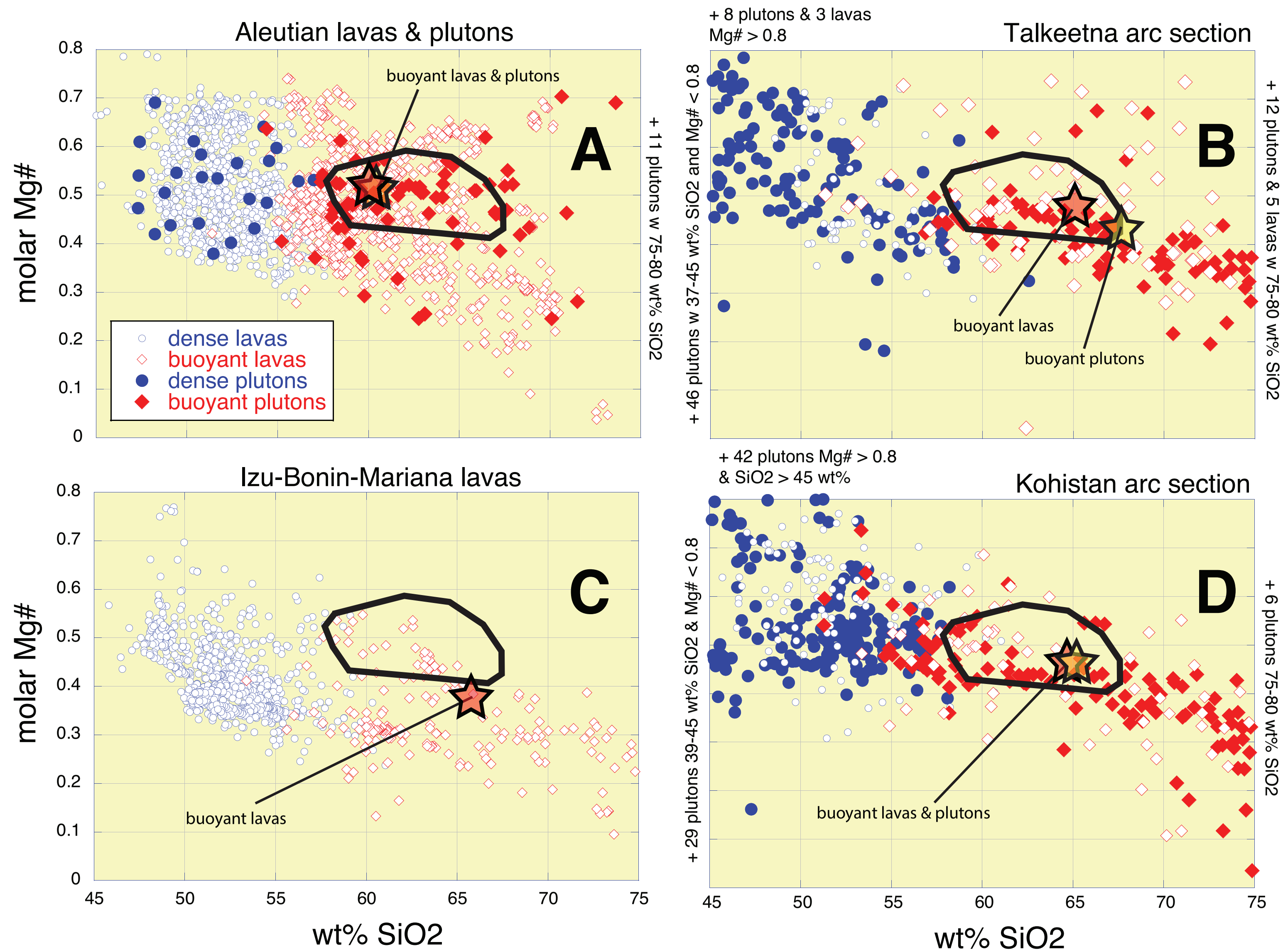

Kelemen & Behn Supplementary Figure S7E-H

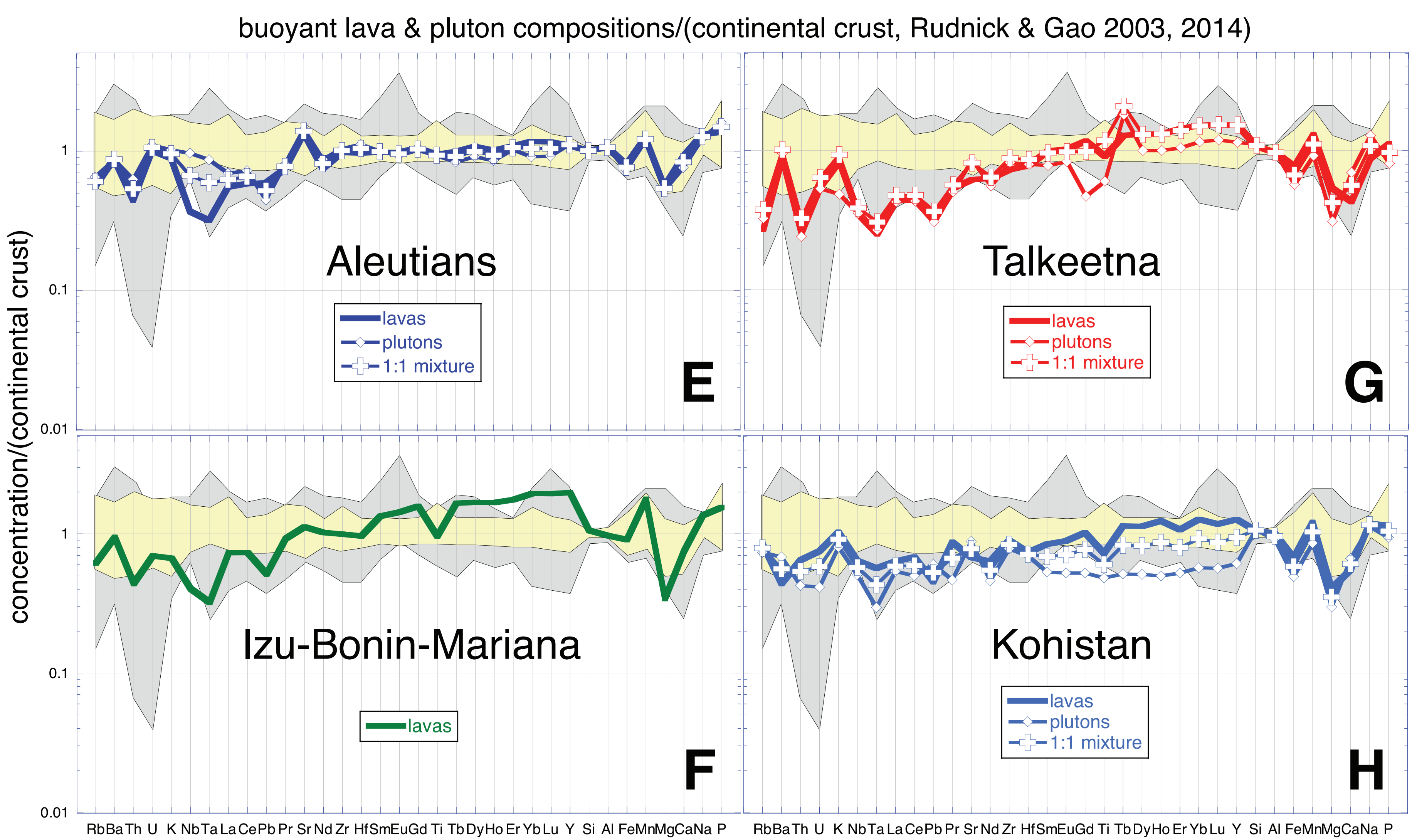

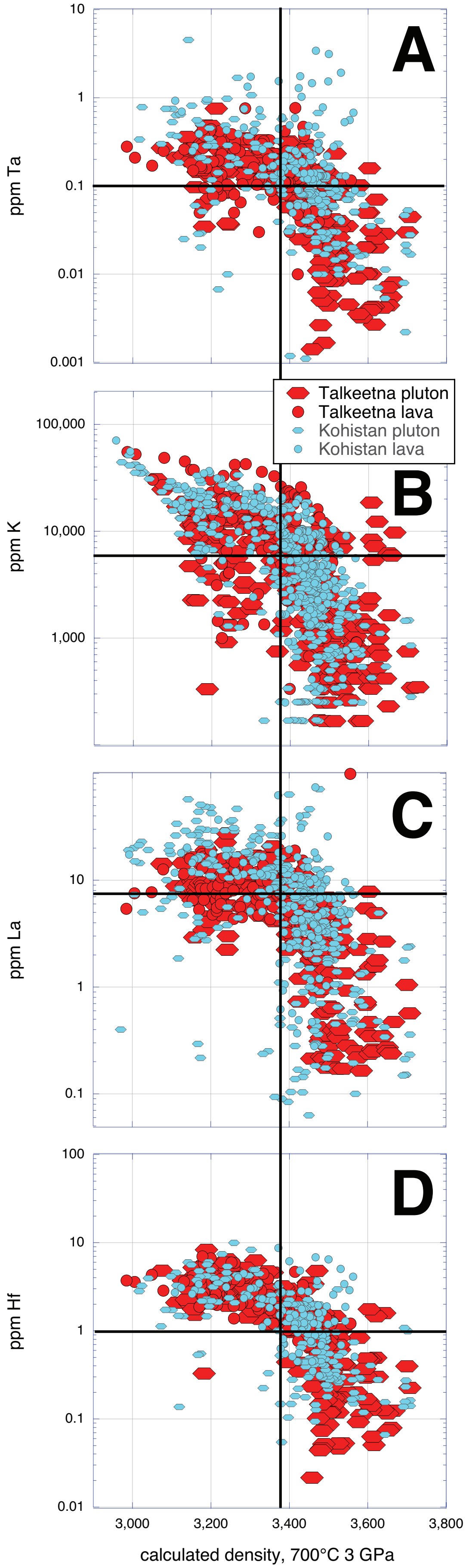

Kelemen & Behn Supplementary Figure S8A-D

Kelemen & Behn Supplementary Figure S8EF